BROADBAND APPLICATION OF

HIGH IMPEDANCE GROUND PLANES

THESIS

Keven J. Golla, First Lieutenant, USAF

AFIT/GE/ENG/01M-11

DEPARTMENT OF THE AIR FORCE
AIR UNIVERSITY

AIR FORCE INSTITUTE OF TECHNOLOGY

Wright-Patterson Air Force Base, Ohio

THE VIEWS EXPRESSED IN THIS THESIS ARE THOSE OF THE AUTHOR AND DO NOT REFLECT THE OFFICIAL POLICY OR POSITION OF THE UNITED STATES AIR FORCE, DEPARTMENT OF DEFENSE, OR THE U.S. GOVERNMENT.

AFIT/GE/ENG/01M-11

BROADBAND APPLICATION OF HIGH IMPEDANCE GROUND PLANES

THESIS

Presented to the Faculty

Department of Electrical and Computer Engineering

Graduate School of Engineering and Management

Air Force Institute of Technology

Air University

Air Education and Training Command

In Partial Fulfillment of the Requirements for the

Degree of Master of Science in Electrical Engineering

Keven J. Golla, B.S.E.E.

First Lieutenant, USAF

March, 2001

AFIT/GE/ENG/01M-11

BROADBAND APPLICATION OF HIGH-IMPEDANCE GROUND PLANES

Keven J. Golla, B. S. E. E.
First Lieutenant, USAF

Approved:

Maj. Peter Collins (Chairman)	6 MAR 01 Date
Maj. Thomas Reid	6 Mar 01 Date
Dr. Andrew Terzuoli	6 Mar 01 Date

Acknowledgements

I wish to thank everyone who helped me complete this research. Special recognition goes to my thesis advisor Major Peter Collins (AFIT/ENG) and sponsor Dr. Stephen Schneider (AFRL/SNRP) who offered me great support and guidance. Their genuine interest and desire to teach make research something I want to continue. I also wish to recognize my other committee members Dr. Andrew Terzuoli and Maj. Thomas Reid whose oversight and recommendations helped validate my findings.

I want to thank Mr. Charlie McNeeley (AFIT/ENG), whose data collection programs and assistance allowed me to take more data than I know what to do with. To Mission Research Corporation for their equipment and thermal imaging technique.

To my classmates Capt. Kyle Freundl and Capt. Alan Dean, who challenged me to stay on course with my thesis yet not become a complete lab-rat.

Finally, with all my heart, I thank my wife and two-year-old son . support and understanding has made the difference between scraping together what I need to graduate and creating a thesis I am proud of. I truly value the opportunity she provided. will no doubt miss visiting me in the "big barn" microwave lab, but I know he has plenty of his own experiments waiting for daddy.

Keven J. Golla

Table of Contents

List of Figures

List of Tables

Abstract

Electrical conductors have long been the only materials available to antenna designers for reflecting structures. However, recently reported high impedance ground plane (HIGP) structures offer a possible alternative. Within a limited frequency stop-band, the high impedance structures create image currents and reflections that are in-phase with a source rather than out-of-phase as for a PEC surface. Also, the high impedance structures suppress surface waves while surface waves propagate on PEC surfaces.

This research explores broadband antenna applications for HIGP structures. A broadband surface mount antenna is applied to both a homogeneous narrowband HIGP and a spatially varying broadband HIGP design. Measurements reveal the ground plane alters the fundamental radiating modes of the antenna and show high frequency regions of the ground plane short out low frequency energy in the antenna.

Novel integrated antenna/ground-plane structures are also introduced and analyzed. Basic high impedance elements are linked to form larger broadband antenna elements within the ground plane itself. The antenna/ground-plane structure becomes a broadband receive antenna that can be fully integrated into a PEC ground plane surface.

1. Introduction

Antennas are invaluable to modern communications and information systems. Wireless telecommunications, global satellite communications, and GPS navigation systems have become as important to commerce and military operations as more traditional radio, TV, and radar systems. Antenna technology has matured to the point where most antenna applications can be filled by off-the-shelf designs or designs created using "cook book" instructions. However, many antenna designs suffer from fundamental material limitations. Metals are indispensable as radiators and dielectrics provide isolation, but no material ideal for all reflector applications has been developed. While perfect electric conducting (PEC) reflectors and ground planes can be practically engineered for most applications, size and performance demands make their integration with PEC antennas increasingly difficult. Recent developments in photonic bandgap technology offer one possible alternative in the form of structures that exhibit high impedance for electromagnetic waves. The structures could replace conventional PEC reflectors and ground planes, while providing the antenna engineer with a new degree of freedom when designing antenna systems.

1.1. Background

Electrical conductors have long been the only materials available to antenna designers for reflecting structures. However, using the same conducting materials for both the antenna's radiating elements and the reflecting ground plane requires good isolation between the two. Physical isolation is necessary to keep the PEC reflector from shorting out the radiating elements. Electromagnetic waves incident on a PEC surface are reflected with a 180-degree phase shift. Thus, an antenna placed on or near a PEC ground plane will not radiate because the energy radiated from the antenna elements will be cancelled by the out-of-phase energy reflected from the ground plane. Moving the antenna elements away from the reflecting surface can restore the radiation by making the energy from the elements add in-phase with the energy reflected from the ground plane. Unfortunately, the physical separation required for efficient radiation increases the overall size of the structure and limits the useful frequency bandwidth.

A second factor affecting the performance of PEC antenna-reflector systems is surface wave propagation on the reflector. Because of the finite size of the reflector, surface waves created on the PEC reflecting surface will propagate until they reach an edge or discontinuity and diffract. The diffracted energy interferes with the desired antenna radiation and degrades the overall antenna pattern. The interference can be reduced by increasing the size of the reflecting ground plane or by absorbing the unwanted surface wave energy. However, the remedies are engineering compromises that attempt to compensate for unwanted material characteristics.

A prime example of engineering compromise can be found in modern surface mount antennas. Because antennas cannot be mounted directly on a PEC surface, surface mount antennas must be mounted over a cavity. The PEC cavity must be large enough to avoid creating reflections that cancel the desired signal. The cavity is also usually filled with an electromagnetic absorbing material to destroy cavity resonances that limit bandwidth. The cavity backed surface mount antenna works but is inefficient because much of the energy radiated by the antenna is lost to absorption in the cavity.

1.2. Motivation

Photonic bandgap technology has grown over the past decade to create structures that avoid many of the limitations of PEC reflectors. The structures are characterized by a frequency stop-band in the electromagnetic spectrum. The stop-band allows the structures to be used in a variety of novel applications, including use as high impedance ground planes for reflecting antenna signals. A high impedance ground plane (HIGP) differs significantly from a conventional PEC ground plane when exposed to electromagnetic radiation. The HIGP exhibits high surface impedance to electromagnetic waves within its frequency stop-band while the PEC ground plane exhibits low impedance for all frequencies. The high impedance ground plane is thus defined by two primary characteristics. First, the high impedance surface creates image currents and reflections that are in-phase with a source rather than out-of-phase as for a PEC surface. Second, the high impedance surface suppresses surface waves while they propagate freely on a PEC surface.

The unique behavior of the high impedance ground plane is desirable for antenna reflector applications. Surface mount antennas could be placed directly on the ground plane surface without a cavity and radiate efficiently. However, current HIGPs are usually only effective within a very limited frequency band. Outside of its effective frequency band, the HIGP behaves like a PEC surface. Although the bandwidth limitation restricts HIGP reflector use to specific specialized applications, individual HIGPs have been created for a wide range of frequencies. The creation of a broadband high impedance ground plane capable of replacing electrically conducting ground planes for antenna applications has become realistic.

1.3. Research Goal

High impedance ground plane technology has advanced to the point where it can be engineered into realistic electromagnetic applications. Based on early photonic bandgap work, practical high impedance ground planes (HIGP) have been developed and have seen limited application as narrow-band antenna reflectors. However, most commercial antenna applications require broadband operation. This thesis research seeks to design and demonstrate a high impedance ground plane that can operate within a broad frequency band and improve the performance of a broadband antenna.

1.4. Scope

This thesis research is a hands-on design, fabrication, and test project. Initial investigation provides better understanding of the capabilities of existing HIGPs and how

they work. The initial results and findings are then applied to potential broadband HIGP designs. A broadband log periodic surface mounted antenna provides the basis for the broadband HIGP work. A broadband HIGP design is tailored to work optimally only for the single antenna. The research is designed to culminate with the demonstration of a working broadband antenna/HIGP pair. Success is determined by how well the combined antenna/ground-plane structure performs across the 2 to 18-GHz frequency band. The research does not directly attempt to create a generic broadband HIGP but should provide a methodology for other broadband designs.

1.5. Organization

The thesis is organized as a progression of concepts and experiments, culminating with the demonstrated capability of a broadband radiating structure. Chapter two provides the background upon which the research builds and gives a perspective of what others have accomplished. Chapter three outlines measurements and results designed to characterize the bulk material properties of ground plane samples. The fourth and fifth Chapters explore approaches to marrying a broadband antenna with a high impedance ground plane by first applying preexisting surface mount antenna designs, then by implementing an integrated antenna/ground-plane structure. The results show the development of concepts, and how they were applied to designing and understanding a broadband HIGP solution. The conclusions bring the thesis into focus and provide a basis for future work.

2. Background

A photonic bandgap (PBG) is defined as a band of frequencies in which electromagnetic waves do not propagate. A material with a complete photonic bandgap is characterized as a three-dimensional structure that does not allow electromagnetic wave propagation in any direction within certain frequency stop-bands. Since Yablonovitch [1] first explored taking photonic bandgap technology out of the optical spectrum into the microwave spectrum in 1987, the pace of research has increased rapidly. However, the research has only recently collimated into a body of work and understanding that allows specialization and direct application of the technology to real world problems. Because the characteristics of the high impedance ground plane are so different from normal conducting ground planes, little is known about how to implement it into a broadband design. Therefore, insight into the technology's eventual application requires a careful study of its development and underlying principles. This study provides the foundation upon which a broadband application of the high impedance ground plane can be made.

2.1. Electromagnetic Bandgap

Multi-layered optical coatings are well understood and indispensable for many of today's optical systems. They are based on periodic boundaries between materials of alternating high and low indexes of refraction spaced at quarter-wavelength intervals [2]. The quarter-wave stack exhibits very high reflectance for light within a limited frequency

band dictated by the thickness of the layers and the materials used. However, the greatest limitation of the quarter-wave stack is that the light must enter the stucture at near-normal incidence to the surface. Yablonovitch sought a periodic three dimensional structure that could prohibit electromagnetic wave propagation for all angles of incidence [1]. While Yablonovitch originally sought an optical crystal structure that would improve the Q of a laser cavity, his work proved equally important in creating photonic bandgap structures for a wide range of the microwave spectrum.

2.2. All-Dielectric Photonic Bandgap Structures

In 1991, Yablonovitch *et al.* [3] fabricated a successful PBG structure incorporating a diamond lattice design. Due to the difficulty of creating a crystal lattice with physical dimensions on the order of optical wavelengths, the PBG structure was designed for microwave frequencies. The crystal was manufactured by marking the top surface of a dielectric slab with a triangular array of holes and drilling through each hole three times at 35.26° off normal and with a 120° spacing in azimuth. The resulting structure in Figure 1 was an array of odd-shaped voids or "atoms" in the dielectric block forming the desired diamond lattice crystal.

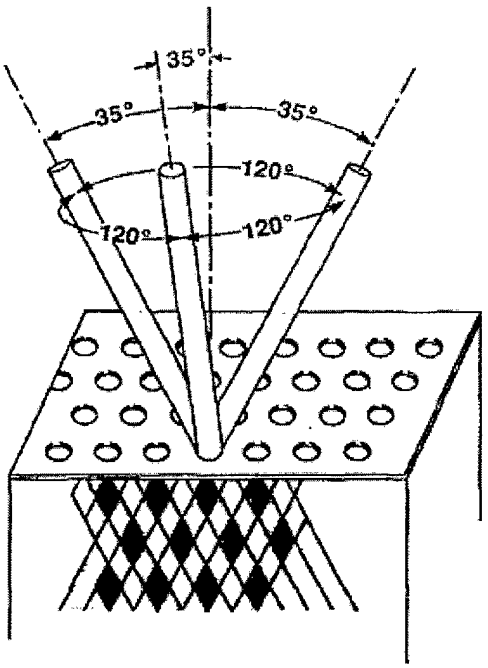

Figure 1. Yablonovite - First Successfully Fabricated PBG Structure [3]

A different curved photonic crystal structure was developed by using Finite-Difference Time Domain (FDTD) computational codes [4]. The structure in Figure 2 was originally modeled in FDTD as a two-dimensional (2-D) parabolic PBG reflector. The FDTD model predicted that the 2-D PBG reflector would provide better gain and beamwidth performance than a metallic reflector. However, a 3-D FDTD model of the entire strucure became too large, so an equivalent surface impedance model was substituted for the PBG reflector. The equivalent surface impedance model provided good agreement with measured results in the narrow photonic bandgap of the reflector.

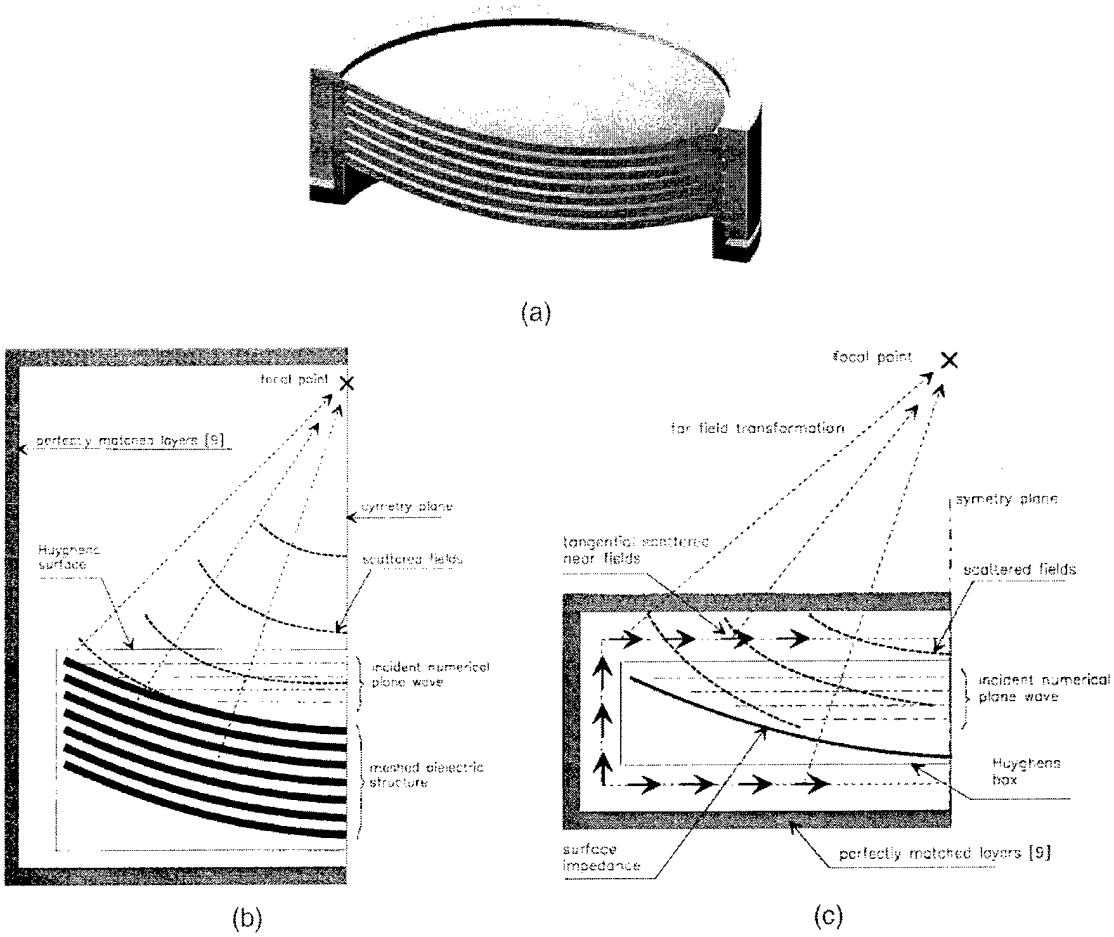

Figure 2. Seven-layer PBG reflector [4]. (a) Transverse view of PBG structure showing alternating layers of dielectric and air, (b) FDTD Computational domain of 2-D model, (c) 3-D model which substitutes an equivalent surface impedance model for the PBG.

2.3. Metallodielectric Photonic Bandgap Structures

The above all-dielectric PBG structures work well but are too bulky and heavy for most practical applications. Metallodielectric PBG structures are capable of reducing the size and weight of the PBG crystal. They take advantage of the capacitive and inductive properties of the metallic elements in conjunction with the dielectric constant of the substrate to tune the frequency bandgap rather than relying on the physical size of the

lattice elements. Thus, the metallodielectric PBG structure can have basic elements and spacings much smaller than the electromagnetic wavelengths it is designed for. Extending the diamond lattice into printed circuit board (PCB) designs, Schloer [5] and Sievenpiper [6] created three-layer crystal structures demonstrating PBG behavior. Both designs in Figure 3 showed evidence of very wide bandgaps for transmission of electromagnetic waves. However, as a reflector, Schloer's design was not able to improve the gain of a broadband antenna beyond that provided by an absorber-loaded cavity [5].

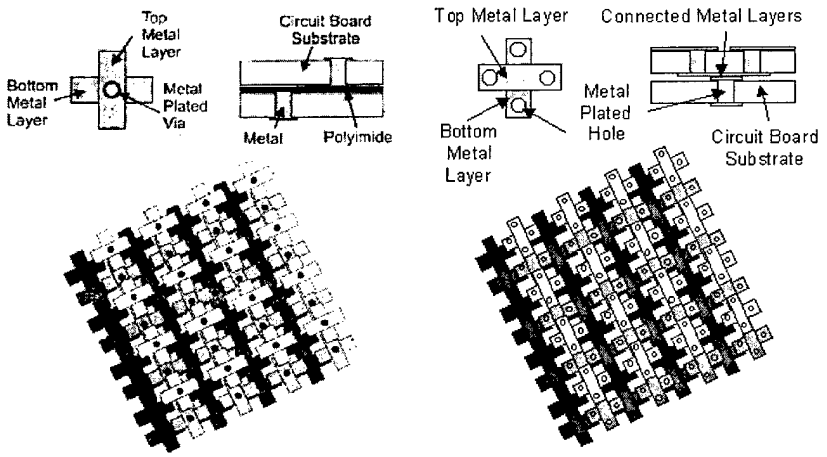

Figure 3. Diamond lattice photonic crystals (PCs) fabricated with printed circuit boards. (a) Metallodielectric PC with metal islands that form capacitive bonds between metal elements [6]. (b) Metallic PC with metal posts connecting the metal elements to form conductive bonds between elements [5].

2.4. Material Modeling Techniques

Although a wide variety of designs exist for PBG structures, similarities in their bulk behavior allow generalized models to be created. In 1996, Kesler *et al.* [7] used the concept of an effective reflection plane (ERP) to describe the total behavior of the

reflected fields from a PBG surface at a particular frequency. The method compares the complex reflection response of the PBG material to the response of a perfect electrical conductor (PEC) reference plane. The result is a measure of how the PBG surface changes the phase of the reflected signal. The phase information reveals the effective "depth" of the PBG material. The ERP model does not fully describe the scattering from the PBG surface, only the combined far-field electromagnetic "appearance" of the PBG surface at certain frequencies.

A second modeling technique describes the behavior of PBG materials by estimating equivalent values for real material parameters. The effective medium theory is useful when the physical size of the PBG material unit cell is much smaller than the wavelength of the desired bandgap frequency. The material is characterized as an effectively homogeneous medium with a frequency-dependent permittivity $\varepsilon_{eff}(f)$ [8]. The effective permittivity estimates the contributions of the individual elements of the inhomogeneous medium as a bulk material parameter. The effective permittivity of the PBG structure can thus be directly compared to the known permittivity of natural materials.

2.5. The High Impedance Surface

The effective medium models provide tools for designing PBG structures to perform specific tasks. In his Ph.D. dissertation [9], Sievenpiper creates the two-dimensional PBG structure or photonic crystal in Figure 5. Rather than characterize the photonic bandgap of the structure, he concentrates on describing and predicting the

effective impedance of the structure surface. By naming the structure a high impedance surface, Sievenpiper highlights the two primary characteristics of the structure. First, the surface creates image currents that are in-phase with a source rather than out-of-phase as for a PEC surface. Second, the high impedance surface suppresses surface waves.

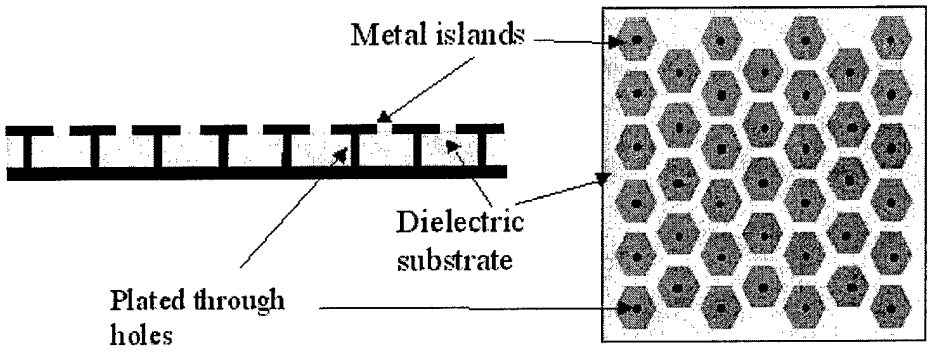

Figure 5. "Thumbtack" high-impedance ground plane [9].

Sievenpiper uses a surface impedance model to predict what physical dimensions on the structure surface will create a desired bandgap width or position on the electromagnetic spectrum[9]. The derivation begins with the surface impedance of a metal sheet, i.e.,

$$Z_s = \frac{E_z}{H_y} = \frac{1+j}{\sigma\delta} \tag{1}$$

where E_z and H_y are the electric and magnetic field components tangent to the surface, σ is the conductivity of the metal, and δ is the skin depth of the metal. However, once capacitive or inductive characteristics are introduced on the surface, the impedance becomes different for transverse magnetic (TM) and transverse electric (TE) modes [9].

$$Z_s(TM) = \frac{j\alpha}{\omega\varepsilon} \tag{2}$$

and

$$Z_s(TE) = \frac{-j\omega\mu}{\alpha} \tag{3}$$

where

$$\alpha \approx \frac{\omega}{c}\sqrt{\frac{\omega\varepsilon}{2\sigma}}(1-j) \tag{4}$$

ω is the frequency in rad/sec, ε is the permittivity constant of the dielectric substrate, c is the free space speed of light in meters/sec, and σ is the conductivity of the metal layer in mhos/square. Equations (2) to (4) show that the surface impedance is frequency dependent and behaves differently for TM and TE modes. Also, an inductive surface with a positive reactance can only support TM waves, while a capacitive surface with a negative reactance can only support TE waves.

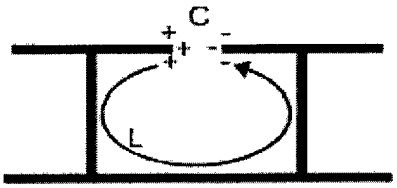

Figure 7. Parallel circuit model of Sievenpiper's patented two layer thumbtack design [9].

Sievenpiper models his thumbtack design as the parallel inductive capacitive (LC) circuit in Figure 7. The inductance is dependent primarily on the substrate material:

$$L = \mu_r \mu_0 t \tag{5}$$

Where μ_r is the relative permeability of the dielectric material (typically assumed equal to 1.0), μ_0 is the permeability of a vacuum, and t is the substrate thickness. The capacitance is dominated by the fringing capacitance between adjacent elements, i.e.,

$$C = \frac{w(\varepsilon_1 + \varepsilon_2)}{\pi} Cosh^{-1}\left(\frac{a}{g}\right) \tag{6}$$

Where w is the edge of an element, ε_1 is the permittivity of a vacuum, ε_2 is the permittivity of the substrate, g is the gap between elements, and a is the center-to-center spacing between the conducting vias [9].

The parallel LC circuit model for the thumbtack design provides a surface impedance equal to

$$Z = \frac{j\omega L}{1-\omega^2 LC} \tag{7}$$

Where L is the inductance, C is the capacitance, and ω is the frequency in rad/sec. The resonant frequency for the LC model marks the high impedance region of the surface. Thus, the resonant frequency is found when the complex part of the impedance equals zero.

$$\omega_0 = \frac{1}{\sqrt{LC}} \tag{8}$$

Similarly, the physical dimensions of the metal pads can be found given a desired center frequency for the high impedance region.

2.6. *The High Impedance Ground Plane*

The significance of the high impedance ground plane (HIGP) follows from its defining characteristics. Because it reflects electromagnetic waves without introducing a phase shift, the HIGP does not require the same quarter wavelength separation from an antenna as a PEC reflector. A radiating element can lie directly adjacent to the surface, while still radiating efficiently [10]. Surface wave suppression also improves antenna performance by reducing interference between antenna elements and by reducing diffraction from the edges of the ground plane itself. The antenna radiation pattern becomes smoother and the antenna radiates more efficiently.

Sievenpiper compared several antenna configurations over high impedance ground planes to the same antennas over conventional ground planes [9]. The HIGP reduced unwanted radiation in the backward direction and smoothed the main lobes for a vertical monopole antenna operating within the HIGP frequency bandgap. The HIGP also improved the directivity of patch antennas. Sievenpiper further demonstrated that a wire antenna could radiate from the surface of the HIGP. Finally, he showed that a HIGP reflector could improve the performance of portable communications antennas by directing the energy away from the user.

2.7. *Conclusion*

The high impedance ground plane is a specialized 2-D application of general 3-D photonic bandgap structures. The HIGP is characterized by its ability to suppress surface

waves and reflect electromagnetic waves without introducing a phase shift. Because the HIGP's properties are directly opposed to the properties of conventional PEC ground planes, it is uniquely suited for novel electromagnetic applications. A growing body of research demonstrates the HIGP and other photonic crystal structures can improve antenna radiation patterns and efficiencies. Furthermore, photonic bandgap reflectors can be made much smaller and lighter than conventional PEC reflectors. However, more research is needed to improve the bandwidth of the high impedance region. Most modern communications systems require broadband operation. The potential for significant improvements in cost, size, efficiency, and range is large. Individual pieces of the solution have been demonstrated. The technology is available for the broadband application of a high impedance ground plane.

3. High Impedance Ground Plane Characterization

While Chapter 2 provides an outline of high impedance ground plane development, this Chapter concentrates on characterizing ground plane properties. Plane wave reflection properties and surface wave suppression characteristics are explored for existing HIGP designs. The bulk material properties of present narrowband HIGPs must be understood before a design can be developed for broadband applications. Also, in conjunction with reflection and surface wave measurements, the role and importance of conducting vias in the ground plane is evaluated.

The Chapter first outlines a methodology for designing and fabricating HIGP boards. Second, narrowband homogeneous HIGP samples both with and without conducting vias are evaluated against PEC and dielectric plate samples. Three different measurement techniques are employed to characterize ground plane performance. Plane wave reflection measurements define frequency bandwidth limitations, surface wave propagation measurements highlight the role of conducting vias, and radar cross section measurements help visualize ground plane scattering mechanisms.

3.1. Ground Plane Fabrication

Previously reported high impedance ground planes were fabricated using electroplated through-vias and chemical etching techniques. The process works but is expensive, slow, and subject to manufacturing errors for some detailed designs. This Section outlines a fabrication process using conductive epoxy vias and a computer

controlled printed circuit board (PCB) milling machine. The proposed process allows rapid in-house prototyping and control over ground plane fabrication tolerances.

3.1.1. HIGP Design.

The narrowband homogeneous high impedance ground plane design is based on Sievenpiper's work described in Section 2.5. The basic "thumbtack" geometry can be seen in Figure 8.

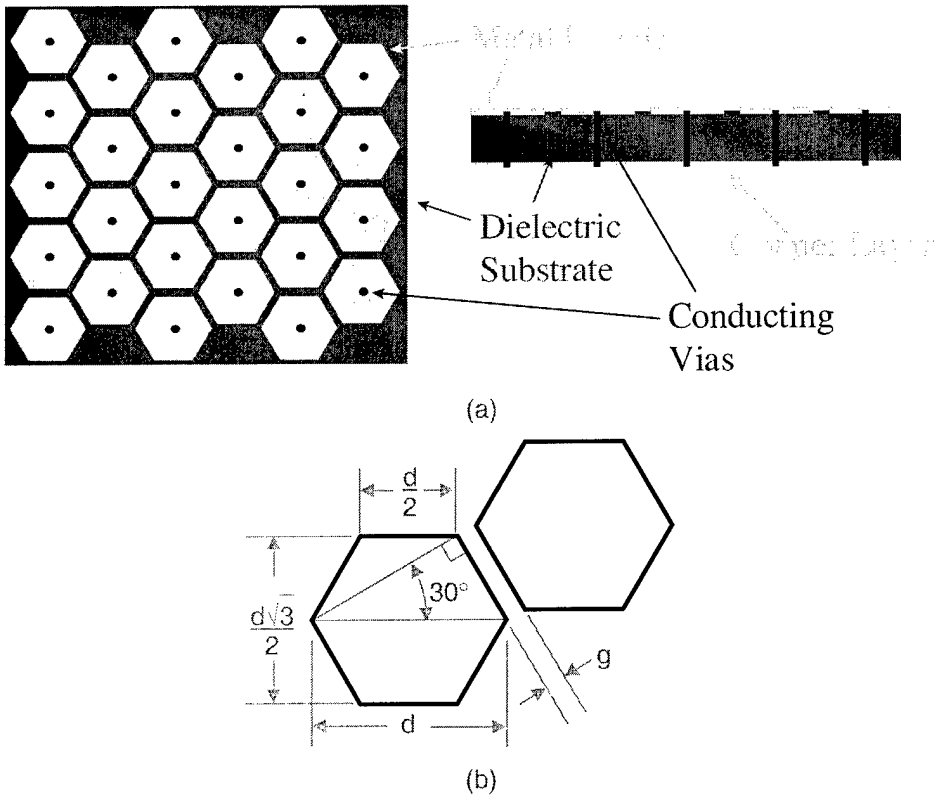

Figure 8. Hex pattern high impedance ground plane. (a) Ground plane milled from printed circuit board (PCB) material. (b) Hex pad geometry.

Recall Sievenpiper calculated the resonant frequency for the hex pattern HIGP by applying an effective surface impedance model. Equation (8) gave the resonant

frequency in terms of the inductive and capacitive properties of the ground plane elements.

$$\omega_0 = \frac{1}{\sqrt{LC}} \tag{9}$$

when

$$L = \mu_r \mu_0 t \tag{10}$$

$$C = \frac{w(\varepsilon_1 + \varepsilon_2)}{\pi} Cosh^{-1}\left(\frac{a}{g}\right) \tag{11}$$

Where μ_r is the relative permeability of the dielectric material (assumed equal to 1.0), μ_0 is the permeability of a vacuum, and t is the substrate thickness. Also, w is the edge-length of an element, ε_1 is the permittivity of a vacuum, ε_2 is the permittivity of the substrate, g is the gap between elements, and a is the center-to-center spacing between conducting vias [9].

Standard double-sided FR-4 PCB material is used for milling the ground planes. Thus, the substrate thickness is t = 59-mils (1 mil = 0.001 inch = 25.4 μm), and the dielectric constant becomes $\varepsilon_2 = 4.9$. Based on the geometry in Figure 8 (b), where d is the hex pad point-to-point diameter, one pad edge is $w = d/2$, and the center-to-center spacing becomes $a = d\cos(30°) = (d\sqrt{3})/2$. Figure 10 plots the HIGP resonant frequency as a function of the point-to-point hex-pad diameter (d) and selected element gap-widths (g).

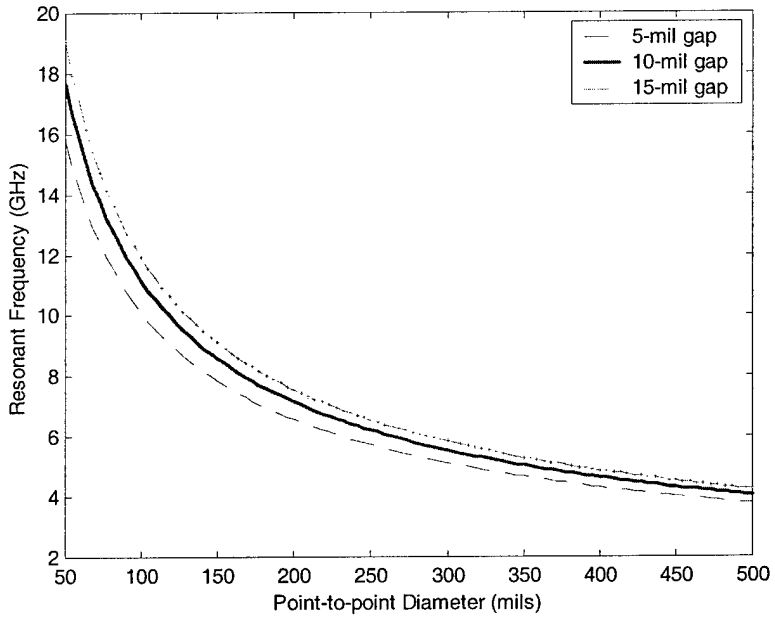

Figure 10. Hex pattern HIGP resonant frequency curves.

A single element gap size and hex pad diameter is used for all of the ground plane characterization experiments in Sections 3.2 to 4.2 below. The gap between ground plane elements is set at 10-mils as a convenient size for the milling machine, while the hex diameter was chosen to be 120-mils to give a high impedance resonant frequency of about 10-GHz.

3.1.2. Fabrication Techniques.

The high impedance ground plane plates are all milled from double-sided FR-4 printed circuit board material with a computer controlled PCB milling machine. However, due to the intricate nature of the HIGP designs and the need to create thousands of individual ground plane elements, several special fabrication techniques were developed.

3.1.2.1. Layout.

Before the ground plane can be physically milled, the HIGP design must be converted to a programmed layout for the milling machine to follow. Because almost ten thousand 120-mil diameter hex pads fit on a 10-inch square plate, the routing path taken by the milling machine becomes very important. Thus, rather than render the ground plane in a CAD program as an array of hex pads, a simple PCB layout program was used to render the ground plane gaps. Also, the milling path was directly programmed to make long continuous horizontal and vertical zigzag-like cuts to help minimize the milling time.

3.1.2.2. Creating Conducting Vias.

A conductive epoxy is used to form the vias that connect the HIGP surface elements to the copper ground plane below. The epoxy is a silver-filled epoxy made by Epoxies Etc. (#40-3905). The cured epoxy has a published volume electrical resistivity of less than 1×10^{-4} ohm-cm.

The first step for creating HIGPs with vias is to drill all the holes in the PCB material with the milling machine. Once the holes are all cleared of debris, and the plate is cleaned, a thin piece of PCB material is used as a squeegee to force the silver impregnated epoxy through all of the vias. When all of the vias are filled, both sides of the board are lightly scraped to clean off excess epoxy and the board is allowed to cure.

3.1.2.3. Milling Ground Plane Surface.

After the conductive epoxy is dry, the board is cleaned and smoothed with a mild abrasive pad. Finally, the board is placed back on the milling machine and the HIGP elements are milled into the PCB surface. Once the ground plane geometry is complete, the ground plane is cut to the final 10"x10" square shape. The surface pads are all isolated from each other on the ground plane surface, but are individually connected to the copper ground plane on the backside of the board by the electrical bond of the conductive epoxy. Continuity tests were performed randomly across the ground plane surfaces to ensure the elements with vias had a DC connection to ground while the elements with no vias were completely isolated. Figure 12 pictures portions of the final HIGP surfaces, one with the conducting vias, and one with no vias.

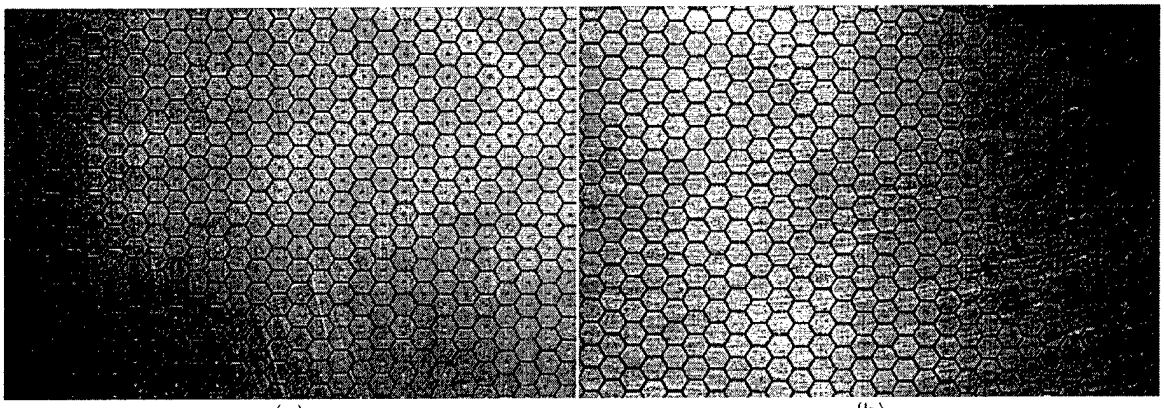

Figure 12. Samples of hex pattern high impedance ground planes milled from PCB material. (a) HIGP with conductive vias. (b) HIGP with no vias.

3.2. Plane Wave Reflection Measurements

As introduced in Chapter 1, the first defining characteristic of a high impedance ground plane is its ability to reflect electromagnetic waves without introducing a phase shift like the 180-degree phase shift created by PEC ground planes. The resulting high impedance reflection coefficient of +1 is exactly opposite the –1 reflection coefficient for a PEC surface. Because a PEC surface exhibits the same 180-degree phase shift for all reflected frequencies, straightforward broadband material characterization can be performed by comparing the reflection properties of the material under test to those of a PEC sample. Thus, the measurement requires a coherent measurement system that records the amplitude and phase of the reflected signal.

3.2.1. Measurement System.

Plane wave reflection measurements were taken at Air Force Research Lab, Sensors Directorate (AFRL/SNS). The ground plane samples were mounted on the lab's focused beam arch, built by the Georgia Tech Research Institute (GTRI). The focused beam arch is a computer controlled network analyzer based measurement system. The GTRI arch uses large dielectric lenses to collimate the energy from horn antennas into a planar wave front on the test sample. The system is capable of making transmission measurements as well as both monostatic and bistatic reflection measurements. Figure 14 shows a typical test setup.

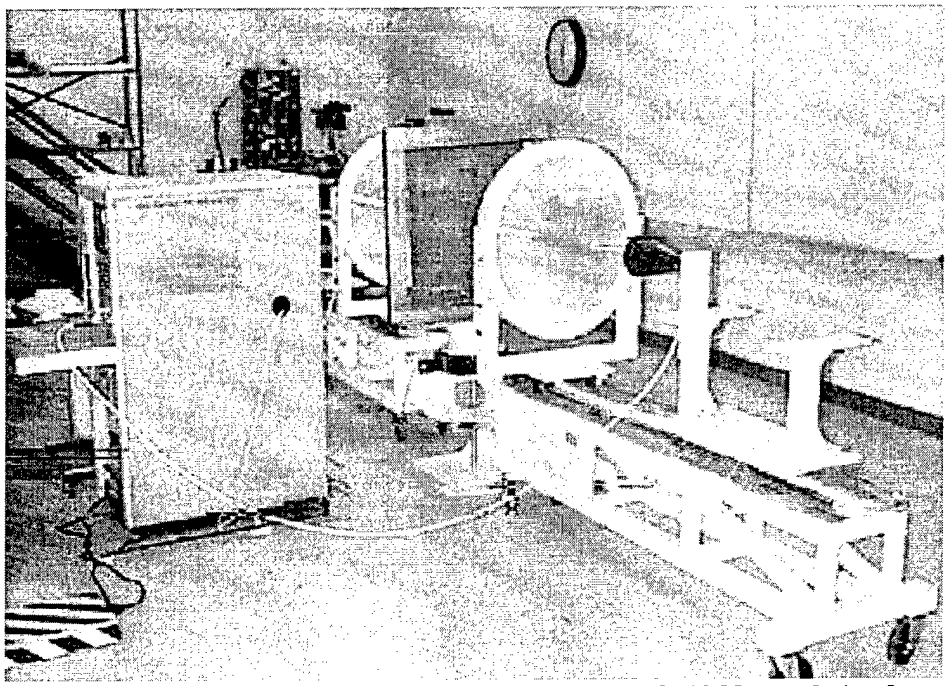

Figure 14. GTRI Focused beam system connected to HP8510 Network Analyzer. As shown, configured for normal incidence reflection and/or transmission. Courtesy, Signatures Technology Branch, Air Force Research Laboratory.

The focused beam system was used to take reflection measurements in two configurations. Both monostatic S11 measurements and bistatic S21 measurements were performed for the ground plane samples. For both configurations, a 10-inch square PEC plate was first mounted in the sample position to perform a measurement calibration. Thus, subsequent frequency response measurements were automatically referenced to the known PEC plate response.

Two narrowband high impedance ground plane samples were characterized on the focused beam measurement system. Both samples are based on the 120-mil hex diameter design described in Section 3.1 above and were fabricated as 10-inch square ground planes from FR-4 printed circuit board (PCB) material. The first sample includes

conducting vias, while the second has no vias connecting the surface hex pads to the ground plane below.

Reflection measurements were performed for each sample while varying three measurement setup parameters. The sample elevation angle (El) was either at 0-degrees normal incidence or at a 45-degree bistatic angle of incidence for each measurement. The azimuth angle (Az) toggled between 0 and 45-degrees changing the orientation of the hex pattern on the sample relative to the antenna polarity. A sample at 0-degrees azimuth is square to the floor while a 45-degree azimuth places the sample in a diamond orientation. Also, all target configurations were measured in both vertical (V-pol) and horizontal (H-pol) antenna polarizations. Table 1 gives the measurement test matrix. Each measurement consists of a coherent frequency sweep from 2 to 18 GHz.

Table 1. Test matrix for focused beam arch reflection measurements.

Sample	*Polarization*	*El Angle*	*Az Angle*	*Sample*	*Polarization*	*El Angle*	*Az Angle*
Vias	H	0	0	Vias	V	0	0
No Vias	H	0	0	No Vias	V	0	0
Vias	H	0	45	Vias	V	0	45
No Vias	H	0	45	No Vias	V	0	45
Vias	H	45	0	Vias	V	45	0
No Vias	H	45	0	No Vias	V	45	0
Vias	H	45	45	Vias	V	45	45
No Vias	H	45	45	No Vias	V	45	45

3.2.2. Reflection Results.

The results of the focused beam arch measurements showed relatively consistent phase and amplitude behavior between the HIGP samples and between different measurement configurations. Both HIGP samples exhibited a phase response that shifted

from 180-degrees out of phase to no phase shift at around 12-GHz. Figure 16 plots the phase response for both samples illuminated with vertical polarization, at normal incidence, and square orientation. Using Sievenpiper's criteria for the bandwidth of the high impedance region [9], the HIGP with vias exhibits a reflected phase shift between $\pi/2$ and $-\pi/2$ over an approximately 3-GHz band. The phase response measurements for all the other sample orientations can be found in Appendix A. Figure 54. Generally, the normal incidence measurements varied slightly with azimuth orientation, while the bistatic measurements varied slightly with polarization.

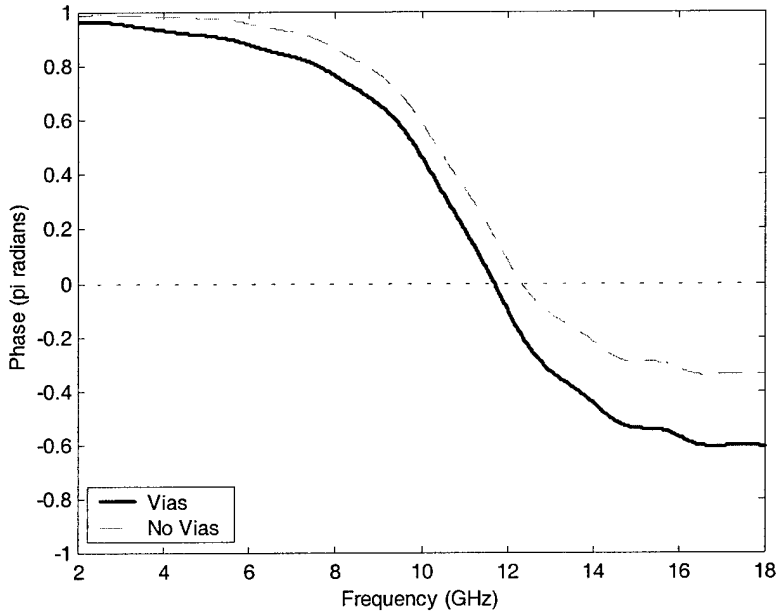

Figure 16. Reflected plane wave phase response for HIGP samples. GTRI focused beam arch, vertical polarization, normal incidence, square orientation.

3.3. Surface Wave Measurements

The second significant characteristic defining the high impedance ground plane is its ability to suppress surface waves. However, it is difficult to measure surface wave propagation across a ground plane. The "AFIT Doghouse" is a specialized test fixture designed to measure surface waves and help characterize the surface wave suppression characteristics of high impedance ground planes.

3.3.1. Methodology.

The doghouse test fixture seen in Figure 11 attempts to isolate two antennas such that only surface wave radiation can be transmitted and received between them. The antennas are designed to launch surface waves for which the electric field is normal to the conducting surface. The antennas are placed on the fixture's curved surface to eliminate line-of-site coupling. Also, electromagnetic absorbing material surrounds the test fixture to reduce noise and multipath coupling. The sample under test is placed in front of the receiving antenna, flush with the conducting surface of the fixture. Each measurement is an S21 network analyzer transmission measurement from 2 to 18 GHz.

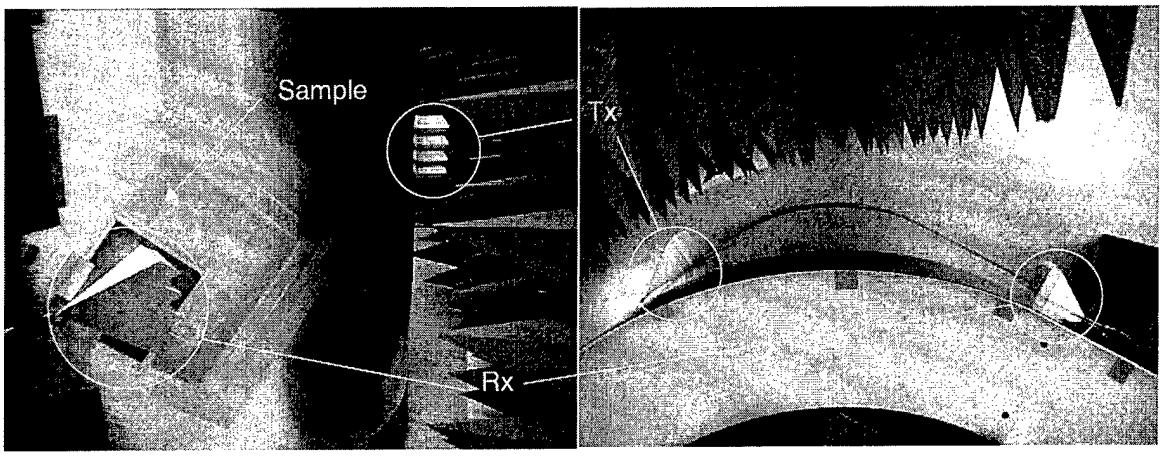

Figure 11. AFIT "Doghouse" setup for surface wave propagation measurements. (a) Side view, showing sample under test. (b) Top view.

The doghouse test setup was used to characterize the surface wave suppression abilities of the two HIGP samples. The measured response from both ground plane samples is compared to the response from a continuous PEC surface. Also measurements are taken with a sheet of magnetic radar absorbing material (MRAM) placed in the sample position. The antennas remain in the same positions for all of the measurements.

3.3.2. Results.

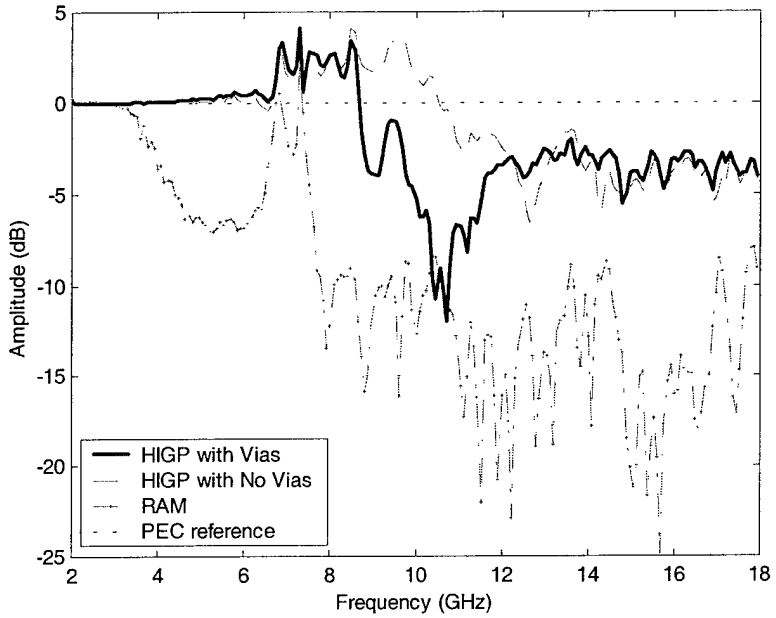

Figure 13. AFIT "doghouse" surface wave measurements taken for different ground plane samples. Frequency response measurements are shown relative to response of continuous PEC surface.

The frequency response plots in Figure 13 show the relative reduction in surface wave propagation for each test sample compared to a PEC surface. The MRAM absorbing sheet introduced a 10-dB reduction in signal amplitude for all frequencies above 8-GHz. The HIGP sample with vias gave a similar 10-dB signal reduction but over a much smaller frequency bandwidth. On the other hand, the HIGP with no vias was not able to reduce the signal by more than 5-dB compared to a PEC surface.

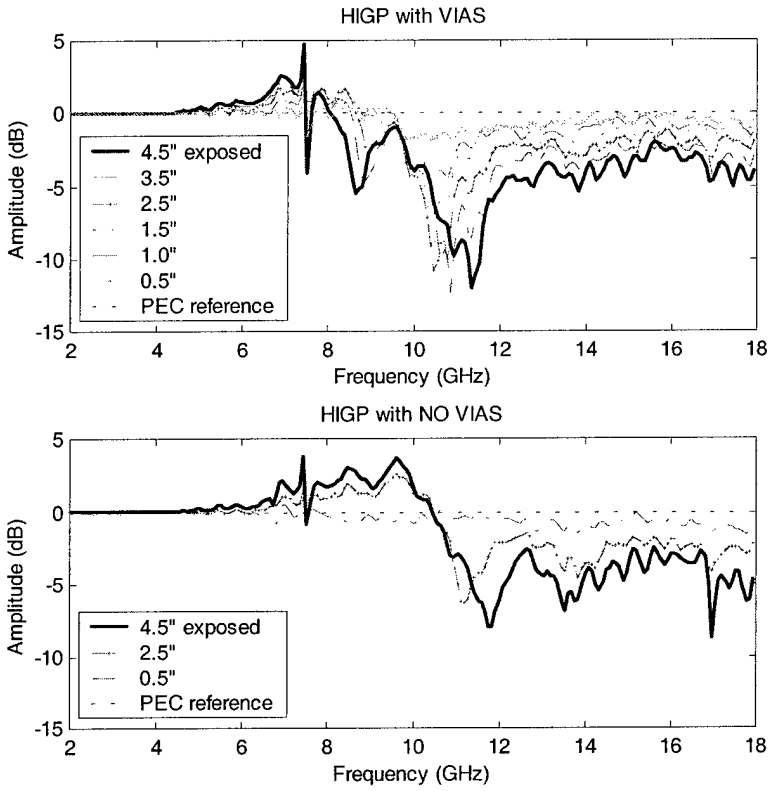

Figure 14. AFIT "doghouse" surface wave measurements comparing frequency response for different widths of exposed HIGP surface. (a) HIGP with vias. (b) HIGP with no vias.

A second series of measurements plotted in Figure 14 give insight into how much HIGP surface area must be present to effectively suppress surface waves. The result shows the HIGP with vias needs to be at least two inches wide to create a frequency stop-band in which surface waves are attenuated by 10-dB. The result also reveals how the HIGP with no vias requires more surface area to maintain its already limited surface wave suppression characteristics.

3.4. Radar Cross Section Measurements

The horizontally polarized monostatic radar cross section (RCS) of an electrically conducting (PEC) square flat plate is dominated by returns scattered from the leading and trailing vertical edges of the plate. Other than at normal incidence, no specularly reflected waves return to the radar from the plate surface. Direct illumination of the leading and trailing edges only creates diffracted returns. However, at near grazing angles, travelling waves on the surface of the plate also create significant monostatic returns. The travelling wave radiation appears in single frequency RCS pattern-cut plots as lobing near edge-on incidence.

Radar cross section measurements offer a tool to help visualize the effects of surface wave propagation on ground plane plates. Coherent RCS data can also be extended to characterize surface wave suppression on a high impedance ground plane. Comparing the relative amplitudes of traveling wave lobes at near grazing incidence can detect the presence or absence of surface wave propagation on ground plane targets. Also, inverse synthetic aperture radar (ISAR) imaging can be exploited for analysis.

3.4.1. Range Configuration.

Measurements were taken in the AFIT RCS range. Four flat square ground plane targets were characterized. All four targets are made from FR-4 printed circuit board (PCB) material as described in Section 3.1.2. The first target exposes the copper side of a 10-inch square one-sided PCB plate, while the second target exposes the dielectric substrate on the other side of the same plate. The third and fourth targets are the same

two HIGP plates used in the reflection and surface wave measurements above. One HIGP target has conducting vias, while the second has no vias. A magnetic RAM sheet is taped to the back surface of all four targets to attenuate creeping waves propagating across the back shadowed side of the plate.

The targets are aligned in the test range as shown in Figure 15, with the top edge level to the ground and the sample surface facing the radar at 0-degrees azimuth. The axis of rotation is along the vertical centerline of each sample. Each measurement includes stepped frequency sweeps of 6.2 to 18.2 GHz in 240 MHz increments for target azimuth positions rotated from 0 to 360-degrees, stepped every 1-degree. Table 3 provides the complete test matrix. Horizontal polarization was used for all measurements.

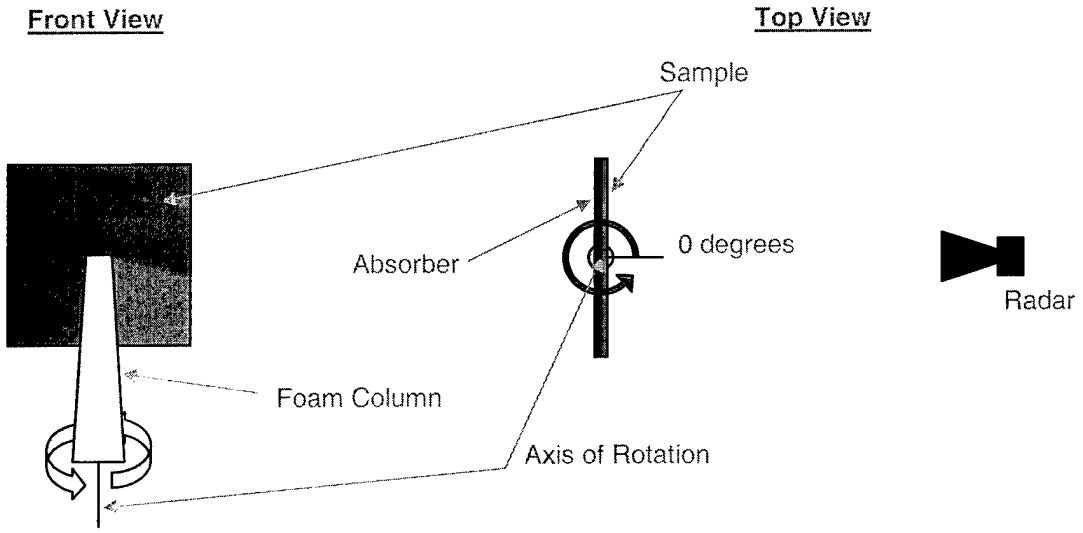

Figure 15. Sample orientation for radar cross section (RCS) measurements.

Table 3. Test matrix for radar cross section (RCS) measurements.

Target	Polarization	Freq. Range / Step (GHz)	Azimuth Range / Step (deg.)
PEC Plate	H	6.2-18.2 / 0.24	0-360 / 1.0
Dielectric Plate	H	6.2-18.2 / 0.24	0-360 / 1.0
HIGP with Vias	H	6.2-18.2 / 0.24	0-360 / 1.0
HIGP with No Vias	H	6.2-18.2 / 0.24	0-360 / 1.0

The RCS measurement system was calibrated using a 6-inch conducting sphere over the desired frequency range from 6.2 to 18.2-GHz. Complete measurement data sets were taken for all four test samples. A complete background subtraction measurement set was also taken for the foam mounting column only. Post-processing was performed using the *MRC Process* software package.

3.4.2. Radar Images.

Each RCS measurement data set creates a two-dimensional complex matrix within which amplitude and phase information is recorded for the entire frequency range at every incident angle. The data can be post-processed to reveal downrange scattering centers and create inverse synthetic aperture radar (ISAR) images. The different RCS images provide different insights into how a target scatters electromagnetic energy. However, note the Fourier transform is an averaging process across the entire frequency band. Thus, narrowband frequency response characteristics can be lost in the downrange and ISAR plots.

3.4.2.1. Amplitude Data.

Figure 17 plots the RCS amplitude data for all four targets after calibration and background subtraction corrections have been made. Relative amplitudes are represented

by different colors at each frequency/position data point creating a two-dimensional color pattern.

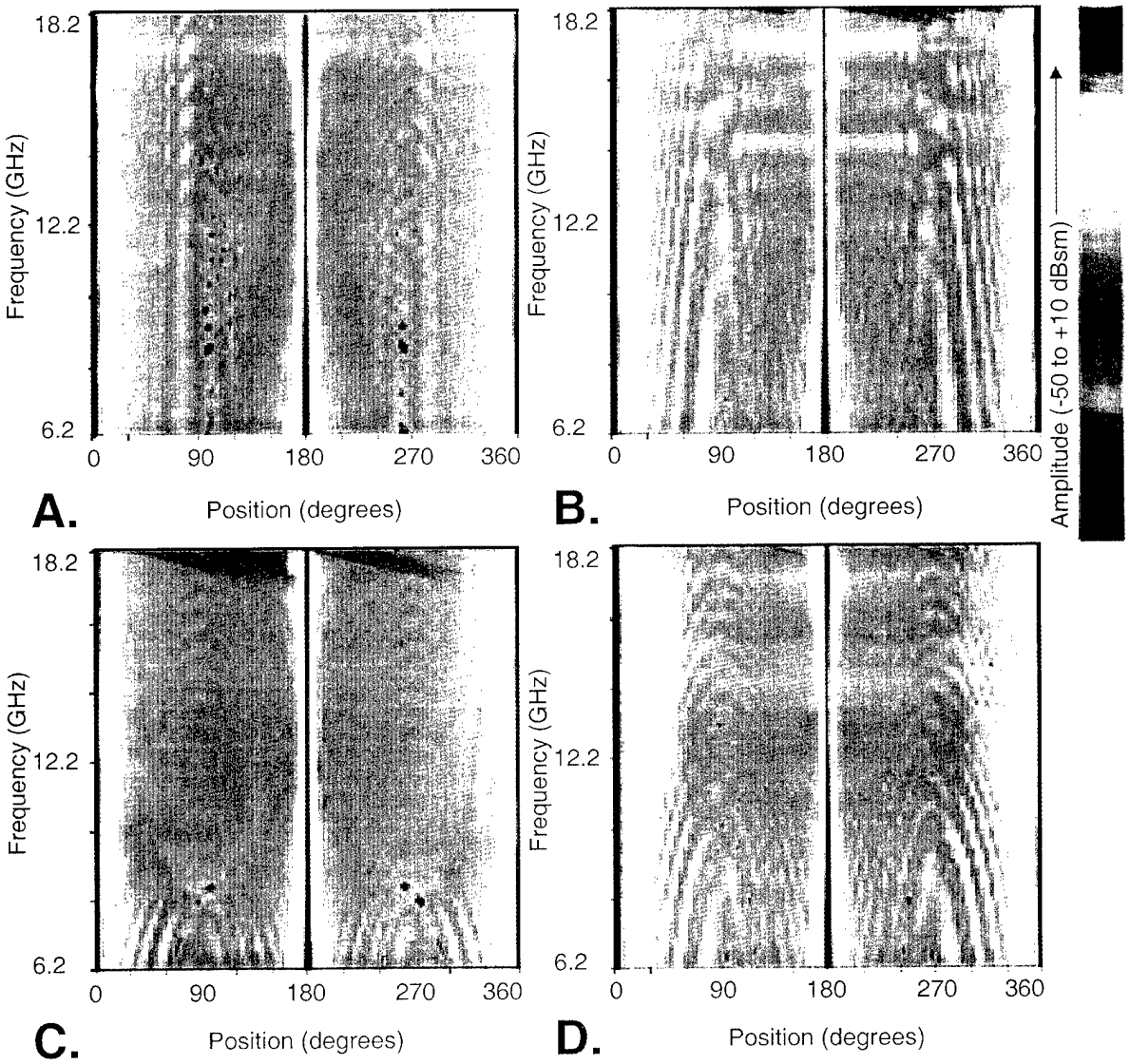

Figure 15. RCS amplitude data plotted as a relative color at each frequency and angular position. (a) PEC plate. (b) Dielectric plate. (c) HIGP with vias. (d) HIGP with no vias.

All four plots show interference patterns caused by diffracted returns from the leading and trailing edges of the samples. Constructive interference ridges are most

visible for lower frequencies and near normal angles of incidence (0, 180, 360 degrees). We expect the diffraction patterns from the illuminated edges to be very similar between samples because the samples are all the same physical dimensions. Differences between samples become more evident when surface characteristics are considered.

Evidence of travelling waves can be seen at near grazing angles of incidence (90, 270 degrees). The PEC plate response shows the first travelling wave lobe as a nearly vertical ridge starting at about 75 degrees. Higher order lobes are also evident at wider angles from grazing. The most prominent travelling wave lobes are found in the dielectric plate plot. The HIGP with no vias shows some activity, while the HIGP with vias reveals very little traveling wave radiation.

3.4.2.2. Downrange Plots.

The first order of post processing RCS data involves applying the Fourier transform over the frequency data for each individual angle position. The result is a downrange image of the scattering centers for each incident angle. Figure 19 presents the combined downrange plots for each of the samples. Color differences again represent signal amplitude. The vertical axis represents the relative downrange distance between scattering centers, while the horizontal axis is target position or angle of incidence.

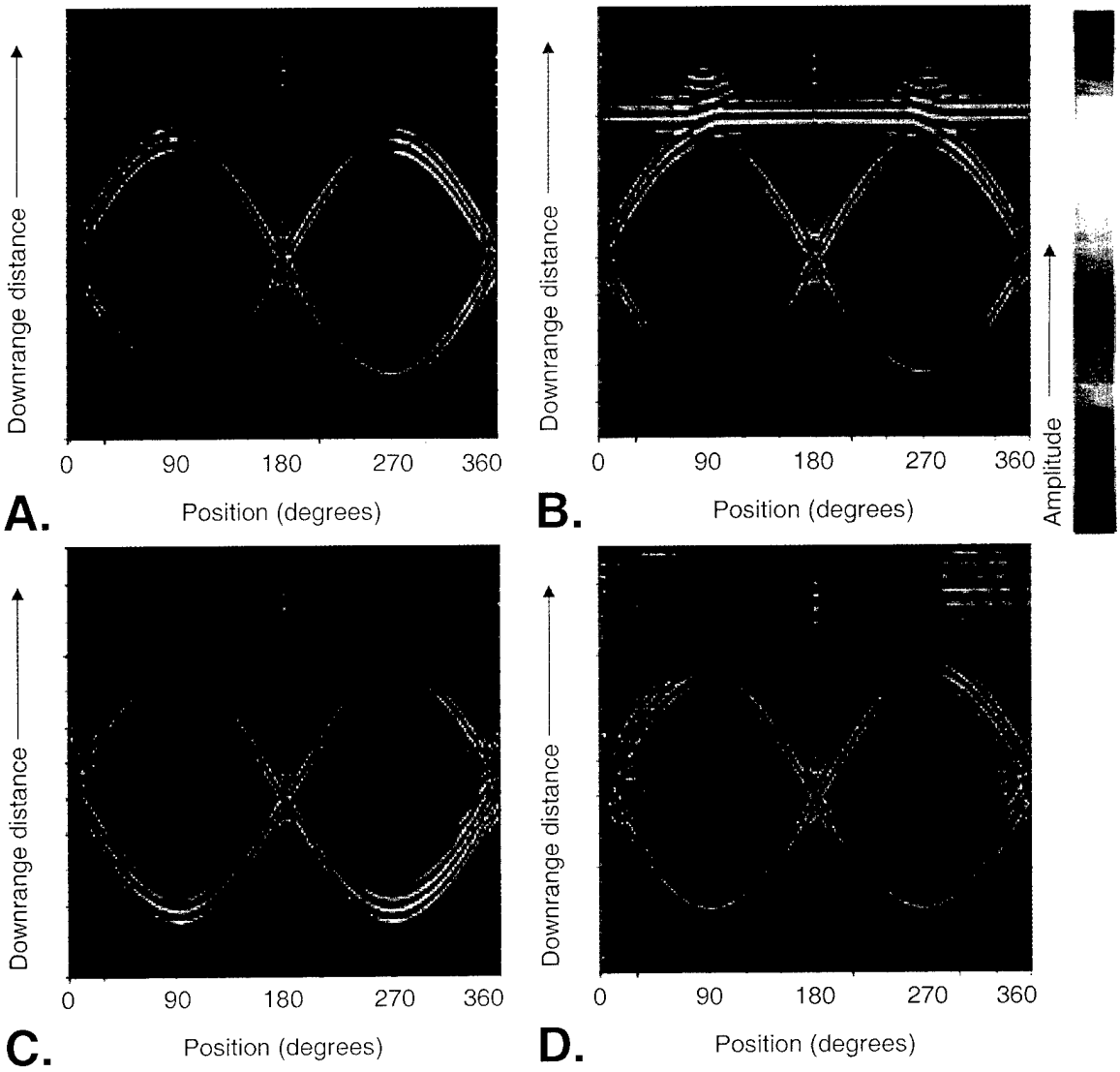

Figure 16. Downrange amplitude plots resolve downrange scattering centers at each angular position. (a) PEC plate. (b) Dielectric plate. (c) HIGP with vias. (d) HIGP with no vias.

Energy scattered from the leading and trailing vertical edges of the samples forms the figure eight patterns. The plots reveal the relative downrange distance between the leading and trailing scattering centers at each angular position. Only one large scattering center is visible when the samples are aligned broadside to the radar. As the samples turn

toward grazing incident angles, the relative downrange positions of the leading and trailing edges grow wider apart.

The PEC plate, dielectric plate, and HIGP with no vias produce very similar plots in Figure 19. Each of the trailing edge returns appears stronger than leading edge return. The trailing edge appears stronger because it is illuminated not only by direct incidence energy from the radar, but also by energy in travelling waves excited on the sample surface. On the other hand, the HIGP with vias exhibits a stronger relative return from leading edge. The weaker relative return from the trailing edge suggests it is not illuminated by surface waves. The fully exposed leading edge of the ground plane thus presents a larger scattering source than the partially shielded trailing edge.

3.4.2.3. ISAR images.

Completing a second transform on the RCS data across a subset of the angular positions creates resolution in the cross-range dimension. The resulting inverse synthetic aperture radar (ISAR) image presents a two-dimensional picture of the target at a certain angle of incidence. The process can also be repeated over other angular regions. ISAR images for each target rotated 70-degrees off broadside can be seen in Figure 21.

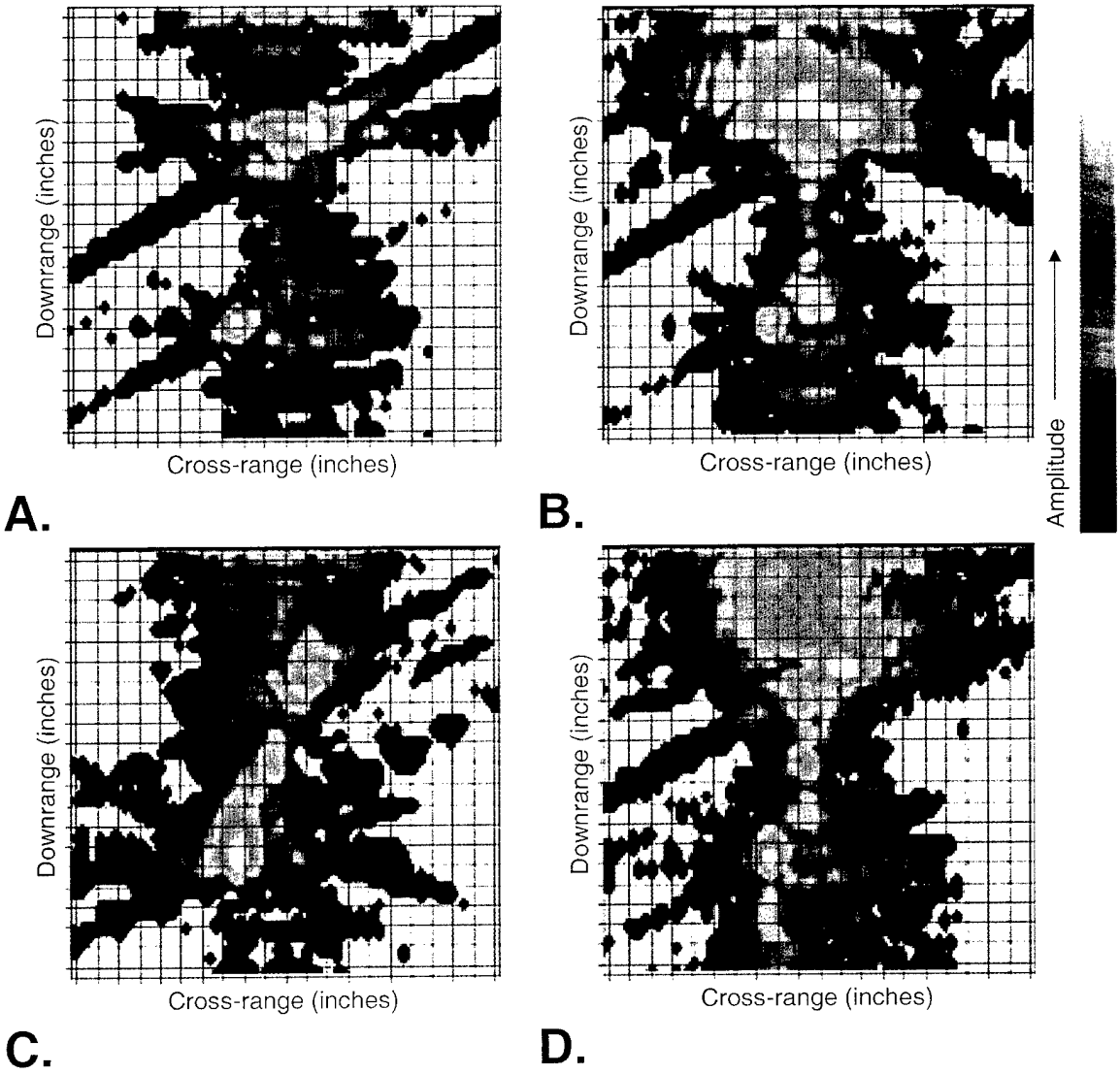

Figure 17. Inverse synthetic aperture radar (ISAR) images for targets at 70° off broadside. (a) PEC plate. (b) Dielectric plate. (c) HIGP with vias. (d) HIGP with no vias.

The ISAR images reinforce the previously drawn conclusions about the scattering centers. The images clearly highlight the leading and trailing vertical edges of each square test plate. The PEC plate, dielectric plate, and HIGP without vias each exhibit stronger scattering from their trailing edge than their leading, while the HIGP with vias

behaves opposite. Also the effects of surface waves can again be seen as energy that appears to come from behind the targets. Because the surface waves are still propagating on the ground planes after the direct illumination scattering has passed, the traveling wave energy gets resolved downrange from directly illuminated returns.

3.5. Conclusion

The above characterization measurements provide good confirmation for the previously reported bulk behavior of high impedance ground planes. Plane wave reflection data shows how the HIGP reflects electromagnetic energy in a narrow frequency band without introducing the 180° phase shift expected from a PEC reflector. Also, travelling wave transmission measurements reveal the HIGP is able to suppress surface wave propagation within its frequency stop-band. Finally, radar cross-section data provides an intuitive comparison of how a HIGP reflects energy versus how a PEC or dielectric ground plane does.

The results show very little difference between HIGPs with vias or without vias for specularly reflected electromagnetic waves. However, the high impedance ground planes do exhibit differences in their ability to suppress surface waves. The HIGP with vias is much more effective at suppressing surface waves than the HIGP with no vias. The results suggest the HIGP without vias allows "ducted" waves to propagate inside its dielectric substrate. By contrast, the conducting vias in the other HIGP block energy propagation within the substrate.

ISAR imaging of ground plane plates provides a potentially valuable tool for characterizing HIGP behavior and bandwidth. However, while the RCS images give a good qualitative feel for how well the HIGP suppresses surface waves, relative to PEC or dielectric plates, they do not provide a good quantitative result. Future measurements could obtain a quantitative result by including an identical, known, but distinct reference target in each ground plane RCS "scene." The resulting ISAR images could be correlated with each other by normalizing the responses to the reference target return.

4. Antenna Reflector Applications

The primary advantage of the high impedance ground plane for antenna applications is the possibility of placing a planar antenna directly onto the ground plane surface. Thus, an antenna/ground plane pair could easily be integrated into the skin of an aircraft or other vehicle without altering the vehicle's internal structure. Present surface mount antennas require a bulky absorber filled cavity behind the antenna surface to operate.

Due to their inherent narrowband nature, present high impedance ground planes have only been applied to improving the performance of matched narrowband antennas. However, different ground planes have been shown to work in different frequency ranges. Broadband HIGP operation can be explored using a planar log-periodic antenna that radiates different frequencies from physically different regions of the antenna. By spatially varying regions of the ground plane to match the active frequency region of the antenna applied above, broadband operation may be possible. A broadband HIGP could be designed in which its narrowband sub-regions locally match the frequency band of the applied antenna.

This Chapter explores the application of HIGPs as reflectors for planar surface mount antennas. The experimental background outlines how a surface mount antenna was chosen, designed, and created and describes the measurement methodology employed to characterize antenna performance. A broadband surface mount antenna is

first applied to an existing narrowband HIGP to provide a foundation for how the ground plane interacts with the broadband antenna. Finally, a spatially varying broadband HIGP is designed and tested.

4.1. Experimental Background

4.1.1. Monopoles.

As mentioned in Section 2.6 above, HIGPs have been successfully used to enhance narrowband antenna performance. Sievenpiper reported improving the performance of a horizontal wire monopole antenna by mounting it over a small square high impedance ground plane [9]. The monopole reportedly radiated over a relatively wide bandwidth, however, at frequencies above the surface wave bandgap of the ground plane, propagating surface waves created many lobes and nulls in the antenna pattern. The monopole radiated most efficiently when the radiated frequency matched the resonant frequency of the ground plane. Sievenpiper also noted the wire antenna should be between a third of a wavelength and a half wavelength long (between $\lambda/3$ and $\lambda/2$) for a smooth radiation pattern and an input impedance near 50Ω [9].

4.1.2. Log-Periodic Zigzag.

4.1.2.1. Theory of Operation.

DuHamel and Isbell introduced log-periodic antennas as structures for which the input impedance and radiation patterns vary periodically with the logarithm of the frequency [11]. The designs grew from research for frequency independent antennas and

self-complementary structures. Although log-periodic antennas are not true frequency independent antennas, the variations in antenna performance over a frequency period can be made small enough that the antenna behaves broadband.

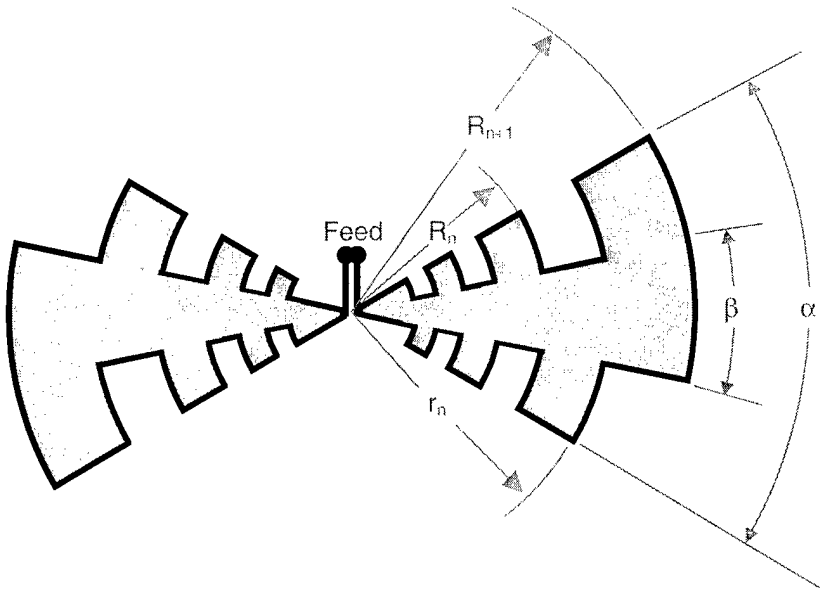

Figure 23. Planar logarithmically periodic antenna geometry.

The basic log-periodic structure seen in Figure 23 can be defined by a set of ratios. The fundamental relationship governing the physical proportions of the log-periodic structure is the geometric ratio τ.

$$\tau = \frac{R_n}{R_{n+1}} \tag{12}$$

The period of operation is also defined in terms of τ. Over the bandwidth of log-periodic antenna, the performance characteristics will be the same for any two frequencies related by an integral power of τ. When plotted on a logarithmic scale, the related frequencies

are equally spaced with a separation or period of ln(τ); hence the name logarithmically periodic structure [11]. The width of the antenna arms or slots is given by:

$$\chi = \frac{r_n}{R_{n+1}} \tag{13}$$

As in Figure 23, χ is usually chosen to be the square root of τ to make the arms and slots proportionately equal. DuHamel and Ore studied the angular parameters α and β but generally found no strong requirements for broadband operation [12]. The sum of the angular parameters α and β should be equal to 90° in order to maintain a self-complementary design. However, DuHamel was able to create working designs where β went to zero. He also showed the shape of the antenna can change if the fundamental log-periodic structure is maintained. Most significantly, DuHamel found he could remove most of the inner area of the antenna conductor without seriously degrading performance. The resulting thin-wire structures perform almost as well as the original planar antennas. Figure 24(a) provides an example of a trapezoidal antenna with its central area removed, creating a thin-wire log-periodic antenna. At one extreme, using triangular elements and shrinking the angle β to zero creates the thin-wire zigzag antenna in Figure 24(b).

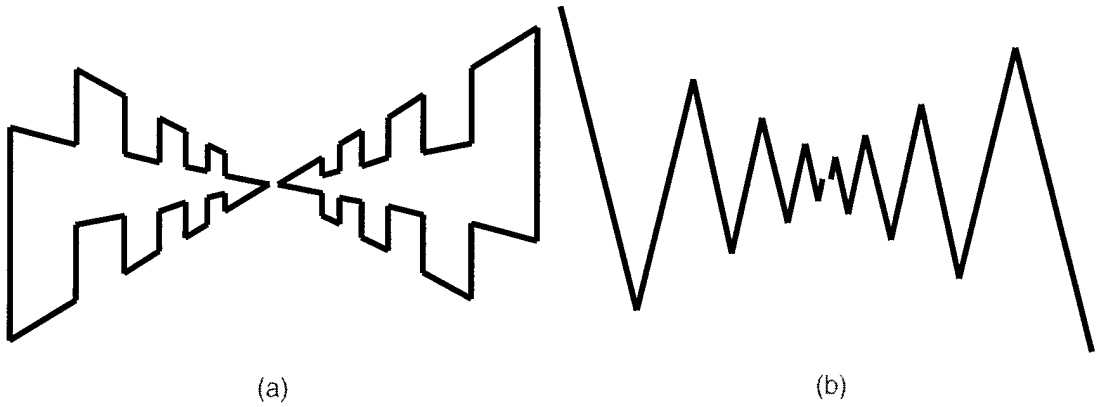

Figure 24. Log-periodic wire antennas. (a) Log-periodic thin-wire toothed trapezoidal antenna. (b) Log-periodic thin-wire zigzag antenna.

The upper and lower cutoff frequencies for a log-periodic antenna are primarily a function of the lengths of the shortest and longest teeth respectively. Generally, the length of the longest tooth corresponds to a quarter-wavelength at the low frequency cutoff, while the length of the shortest tooth corresponds to a quarter-wavelength at the high frequency cutoff. The quarter-wavelength resonant regions also contribute to a distinguishing characteristic of all log-periodic antennas. Currents on the antenna rapidly disappear after progressing past the region where a tooth is a quarter-wavelength long [12]. Thus, for mid-band frequencies, a log-periodic antenna appears to operate differently in three distinct regions. The transmission region in the center of the structure carries low frequency energy out to the radiating elements in the active region. A quarter-wavelength tooth dominates the active region where most of the energy is radiated. The outer antenna elements form an unexcited region because no current is expected to propagate beyond the active region.

4.1.2.2. Design Considerations.

The purpose for using a log-periodic antenna is to provide a broadband tool for characterizing broadband high impedance ground planes. Thus, the antenna must be planar and must fit within the 10-inch-square ground planes. To be an effective broadband diagnostic tool the antenna must maintain a level frequency response (above 0 dBi) across the 2 to 18 GHz band of interest. Finally, the antenna should allow the maximum possible physical space between high frequency and low frequency elements to provide room for differently scaled regions within the corresponding high impedance ground plane.

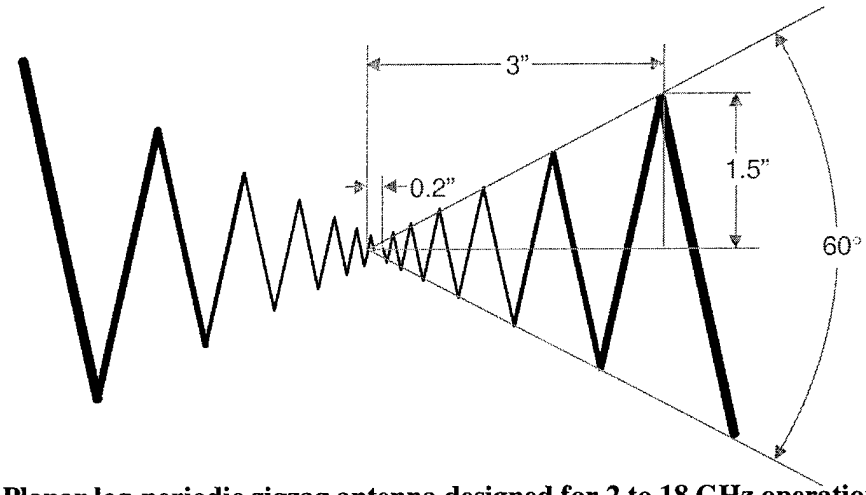

Figure 26. Planar log-periodic zigzag antenna designed for 2 to 18 GHz operation.

The planar log-periodic zigzag antenna in Figure 26 meets the above criteria. A zigzag design was chosen primarily due to the apparent failure of Saville's trapezoidal log-periodic antenna as a high impedance ground plane diagnostic tool [13]. The zigzag design eliminates the need for horizontal connectors between vertical radiating elements.

Also, the simple shape makes milling the small high frequency elements in the central region less delicate. A geometric ratio of $\tau = 0.64$ was used in the design.

4.1.2.3. Fabrication.

The zigzag antennas were originally milled on single sided 31-mil thick (1 mil = 0.001 inch) FR-4 printed circuit board (PCB) material. However, the PCB antenna continues to radiate when it is mounted on a PEC surface. The thickness of the dielectric provides enough space such that the image currents from the PEC surface do not cancel the antenna signal. The antenna begins to operate like a radiating microstrip line. Therefore, the zigzag antennas used in Sections 4.2 below and 4.3 below are milled from 2-ounce copper foil stock (approximately 4-mil thick). A layer of dielectric tape is used to isolate the antenna from the ground plane surface. Also, a layer of dielectric tape is used to hold the foil antenna flat on the ground plane surface. Return loss measurements with other antennas showed the tape did not perceptibly perturb antenna performance. Figure 21 shows a zigzag antenna mounted on a copper plate.

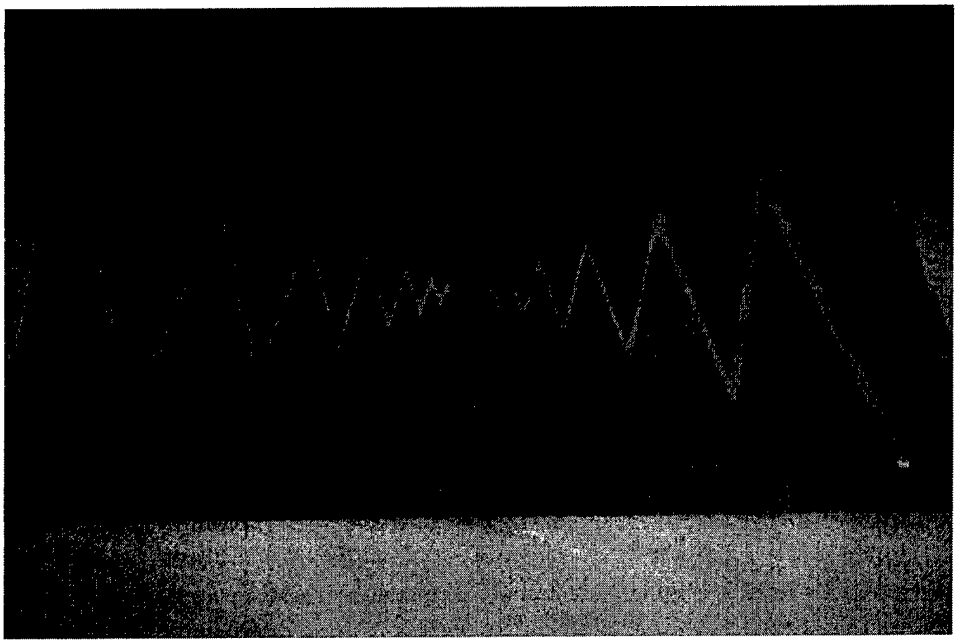

Figure 21. Thin foil planar log-periodic zigzag antenna mounted on copper plate with blue dielectric tape.

4.1.3. Measurement Methodology.

Antenna performance measurements were taken at the AFIT antenna range seen in Figure 23(a). The antenna range is based on an HP8510B Network Analyzer and is computer controlled. Figure 23(b) provides a block diagram of the range setup. Both the frequency sweep and pattern cut measurements are S21 measurements. Channel 1 of the network analyzer drives an HP8349B RF amplifier. The output of the amplifier drives a standard gain horn that transmits into an anechoic chamber. The signal received by the antenna under test is returned to channel 2 of the network analyzer. All antenna measurements are referenced to the corrected measured response of a second standard gain horn. The antenna range also features a computer-controlled turntable allowing the antenna under test to be rotated in azimuth as measurements are taken.

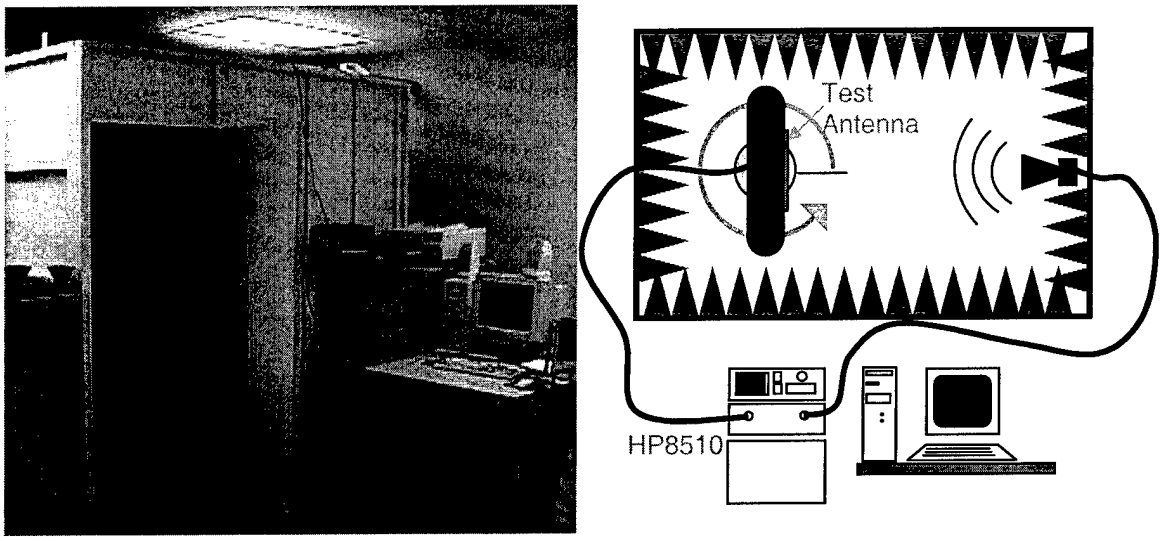

(a) (b)

Figure 23. AFIT antenna test range. (a) Anechoic chamber and instrumentation. (b) Antenna range block diagram.

All antenna measurements were taken with the antennas mounted on a circular test body to limit the effects of edge diffraction and simulate an infinite conducting ground plane. The test body is an 8-inch-thick, 36-inch-diameter conducting disc with all rounded edges. Figure 25(a) shows how the test body is mounted on edge on a foam column inside the AFIT antenna range anechoic chamber. Antennas under test are mounted on one side of the test body over absorber, a copper plate, or a HIGP plate.

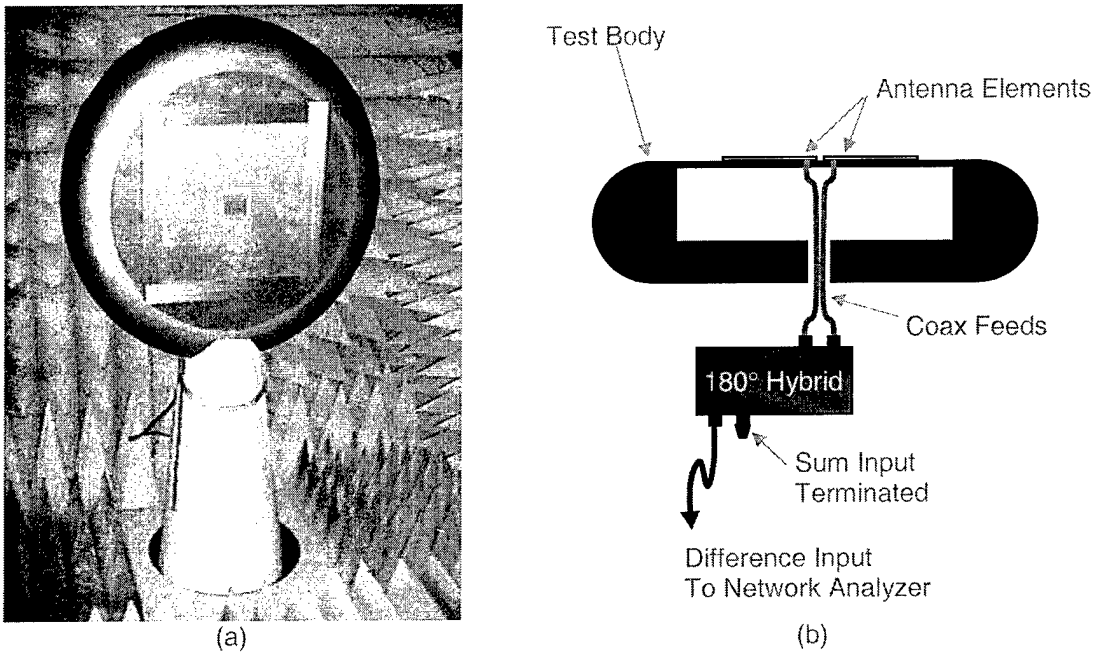

Figure 25. Antenna test body. (a) Test body on rotating foam pedestal. (b) Antenna feed block diagram for two-arm log-periodic antenna.

Figure 25(b) provides a block diagram for how the two-arm planar antennas are fed and mounted. Log-periodic antennas require a balanced feed. Each side of the log-periodic antenna is connected to the center conductor of a semi-rigid coax. The coax lines are connected to the outputs of a 180° hybrid device and the hybrid is fed through its difference input. Also, the outer conductors of the coax feeds are connected to each other and the test body ground plane with copper tape. When the zigzag antenna is mounted over a ground plane, two 90-mil holes are drilled in the center of the ground plane plate for the coax feeds. One-arm antennas are connected directly to the Network Analyzer without the hybrid device.

4.1.3.1. Frequency Sweeps.

Frequency sweep measurements are all taken with the antenna at 0° azimuth (broadside). Data is taken over a 2 to 18 GHz frequency range. The network analyzer is set in the stepped frequency sweep mode with 801 data points over the frequency range and an averaging factor of 64. A post-processing 3 point sliding averaging window is applied to the data for the plotted results.

4.1.3.2. Pattern Cuts.

Antenna pattern-cut measurements are created by taking frequency sweeps while the antenna test body steps in 1° increments rotating from 90° to -90° azimuth. The frequency sweep is taken from 2 to 18 GHz, in stepped frequency mode, with 51 frequency data points and an averaging factor of 64.

Assuming the antenna under test is linearly polarized with the E-field oriented vertically, all of the antenna patterns are H-plane pattern cuts. The transmitting antenna can also be rotated such that its radiated E-field is oriented either vertically or horizontally.

4.1.3.3. Return Loss / Impedance.

The return loss measurements are S11 measurements with the antenna connected directly to channel 1 of an HP8720C network analyzer. Data is taken in stepped frequency sweep mode for 201 frequency points over a 2 to 18 GHz range. Also, the IF

bandwidth is set to 300 Hz, 16 sweep averaging is activated, and the network analyzer is calibrated.

4.2. Narrowband Application

To provide a baseline for designing a broadband high impedance ground plane, the log-periodic zigzag antenna was first applied to a narrowband HIGP. Antenna response measurements contrast how the broadband antenna performs over the narrowband HIGP compared to how it performs over an absorber filled cavity or over a PEC surface. The antenna over absorber measurement represents a typical surface mount application of the antenna. The antenna over PEC ground plane response highlights the frequency band where the HIGP is exhibiting high impedance behavior.

Figure 27 shows the broadside frequency response curves for the zigzag log-periodic antenna mounted over absorber, PEC, or a HIGP. A homogeneous HIGP with conducting vias was used for the narrowband HIGP sample. The frequency sweeps show how the image currents produced by the PEC ground plane reduce the antenna response across the entire frequency band, while the HIGP actually enhances the antenna response by 2 – 3 dB from about 10 to 12 GHz. As expected, the broadband antenna mounted on a HIGP performed better within the ground plane's frequency stop band than the same antenna mounted over absorber. The result also reinforces previous plane wave reflection measurements in Section 3.2.2 showing the HIGP sample has a frequency stop band in the 10 to 13 GHz region. See Section 4.1.3 for details on measurement parameters and setup.

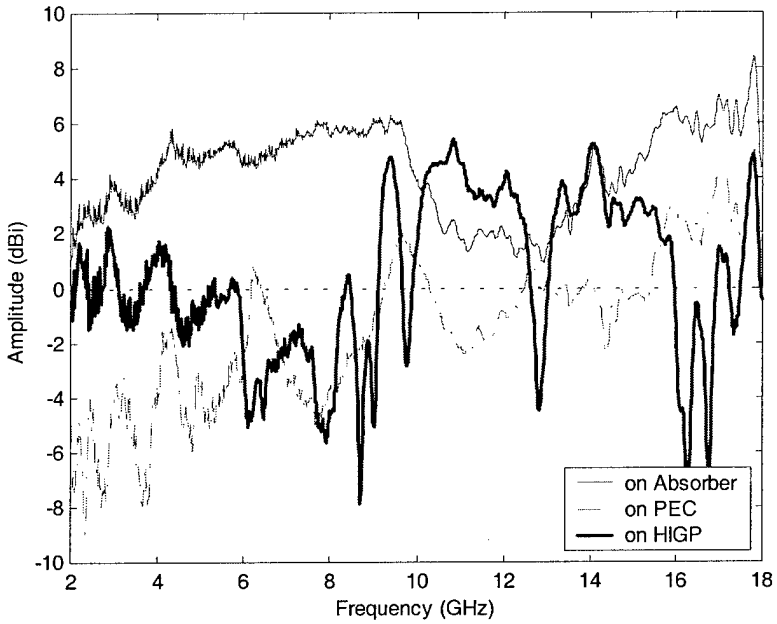

Figure 27. Thin foil log-periodic zigzag antenna mounted on absorber filled cavity, on PEC plate, and on narrowband HIGP. Broadside frequency sweeps.

A second experiment was conducted to help determine the physical region of the zigzag antenna radiating in the frequency stop band of the HIGP. With the zigzag antenna still mounted on the HIGP surface, successive arms or teeth of the antenna were cut off, starting with the larger low frequency arms at the ends. The antenna response within the ground plane stop band should fall off once the actively radiating region of the antenna is removed. The results can be seen in Figure 29. Little change in the overall frequency response is evident until more than half of the antenna is removed. Furthermore, even when only the smallest portion of the original antenna remains intact, the frequency response remains high over a 9.5 to 13 GHz band. The response only disappears when the entire antenna is removed, leaving only the coax leads.

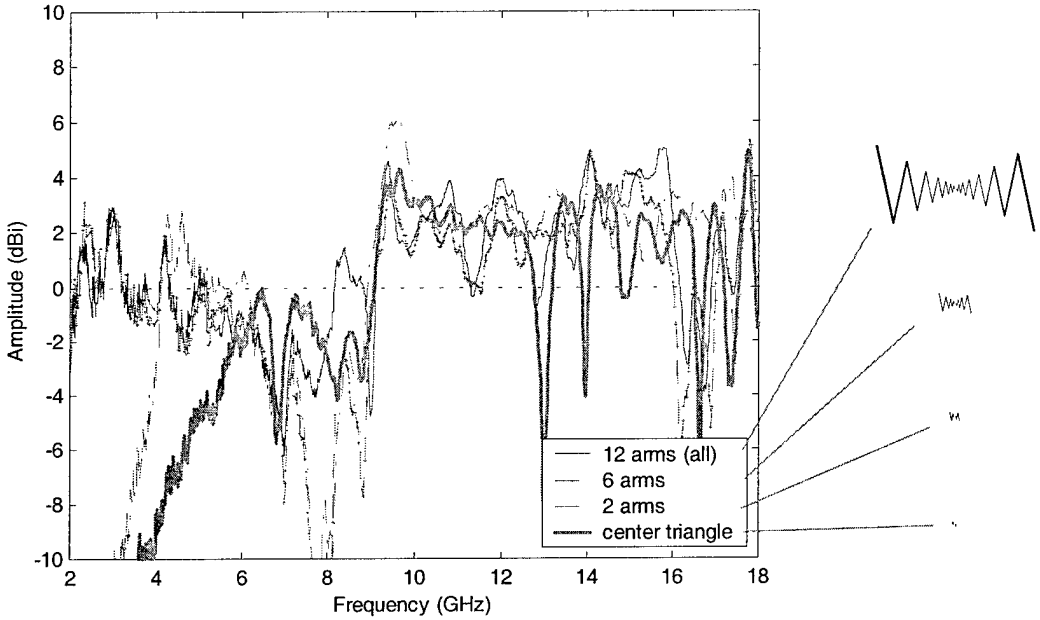

Figure 29. Thin foil log-periodic zigzag antenna on narrowband HIGP with successive arms removed from low frequency region of antenna. Broadside frequency sweeps.

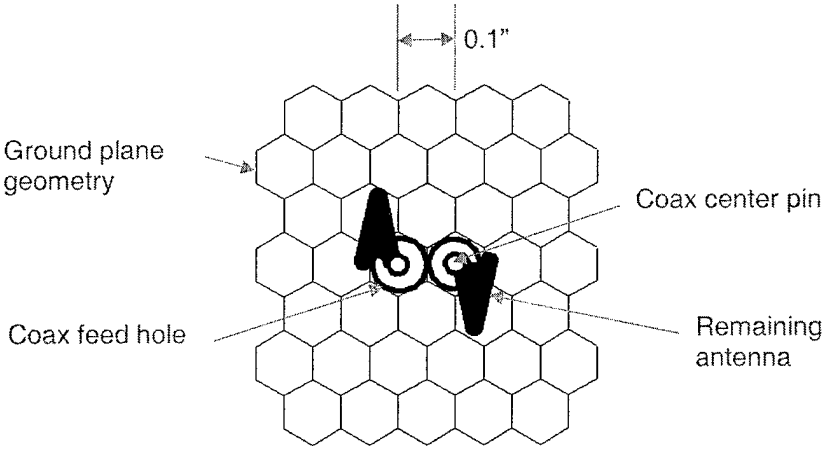

Figure 31. Center triangles of log-periodic zigzag antenna mounted on narrowband HIGP (correct geometric proportions).

Figure 31 clarifies the physical relationship between the center triangles of the antenna, the coax feeds, and the ground plane elements below. The zigzag antenna has been cut down to an array of two small triangular patches. Each triangle covers only two

or three basic elements of the ground plane, yet the pair radiates at wavelengths 6 to 8 times their physical length. The two triangular patches appear to be coupling energy from the active frequency band gap of the ground plane itself.

4.3. Broadband Application

A spatially varying inhomogeneous HIGP was designed for testing the broadband response of combining several locally narrowband high impedance regions into one ground plane. The ground plane is evaluated by its ability to enhance the broadside frequency response of the planar zigzag antenna. While the results from Section 4.2 showed the zigzag antenna no longer behaved like a log-periodic when applied to a narrowband HIGP, the antenna may couple energy from different ground plane regions into a single broadband response.

4.3.1. Broadband HIGP Design.

The broadband HIGP design explores varying the scale of the ground plane elements to match the log-periodic topology of the applied zigzag antenna. Small ground plane elements corresponding to the high frequency region of the antenna transition to larger elements scaled and positioned to match the low frequency regions of the antenna. The radiating elements of the log-periodic antenna grow by a constant geometric ratio as they extend from the center of the antenna, while the radiated frequency decreases on a logarithmic scale. Unfortunately, the physical size of the high impedance ground plane elements do not share the same relationship with their corresponding frequency stop

bands. Recall Figure 10, relating the radius of a HIGP element to the ground plane's resonant frequency.

The physical proportions and spacing of the broadband ground plane regions were chosen using Sievenpiper's effective impedance model described in Section 2.5. The broadband HIGP contains four basic element regions and three transition regions. Using the original narrowband HIGP geometry with a hex-diameter of 120-mils as the fundamental element, one basic element is half its size, one is twice its size, and one is four times its size. The linear relationship between the ground plane elements provides relatively even high impedance stop band coverage across 2 to 18 GHz and allows geometrically simple transitions between ground plane regions. The milled gaps between the ground plane elements remain 10-mils wide throughout the entire board. The ground plane geometry can be seen in Figure 33 along with the applied zigzag antenna.

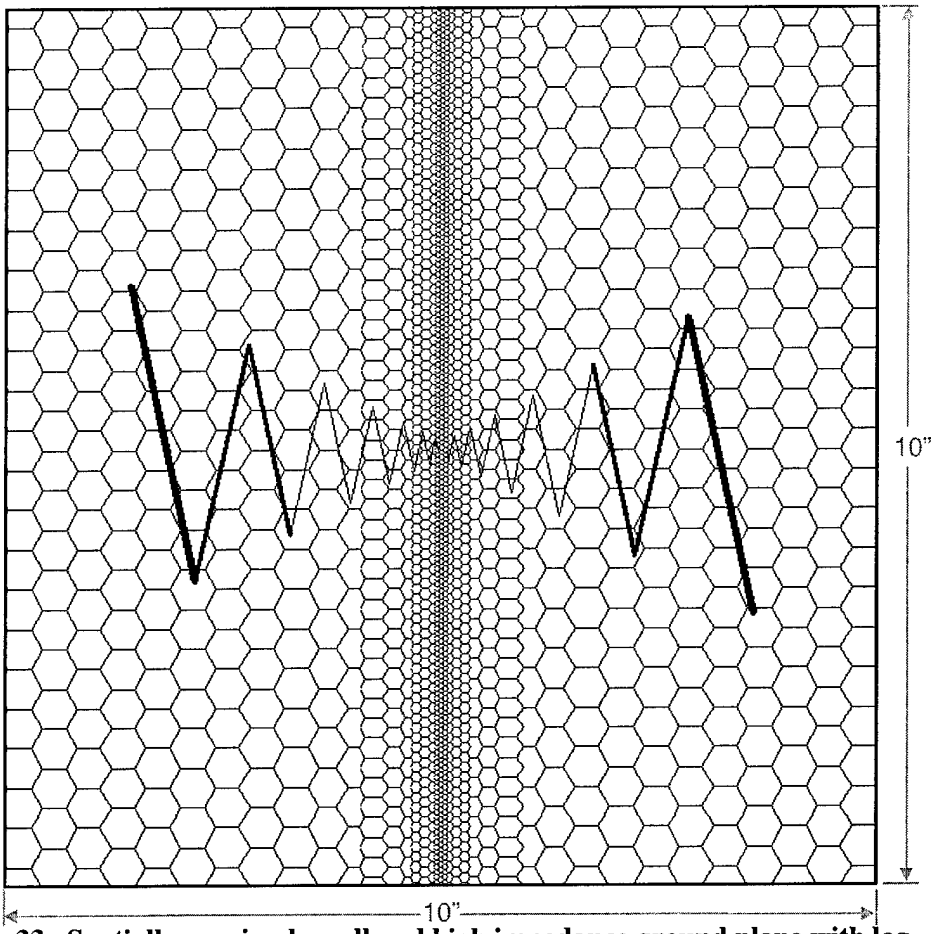

Figure 33. Spatially varying broadband high impedance ground plane with log-periodic zigzag antenna

4.3.2. Zigzag Antenna on Broadband HIGP.

The planar log-periodic zigzag antenna was mounted on the spatially varying broadband HIGP with dielectric tape as explained in Section 4.1.2.3. Figure 33 above highlights the relationships between the ground plane regions and the applied antenna elements. The broadside frequency response measurement for the antenna/ground-plane pair is plotted in Figure 35. The result shows a response for only the highest frequency region. It appears the high frequency region in the center of the ground plane effectively "shorts" the low frequency energy from the other ground plane regions. Energy at

frequencies below the active band gap of the center ground plane elements is not allowed to propagate over them and never reaches the center feeds of the zigzag antenna.

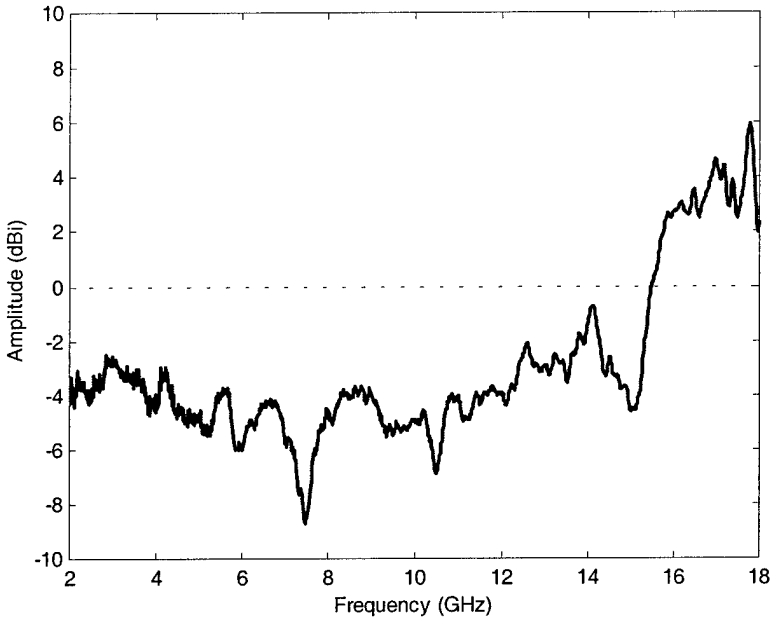

Figure 35. Thin foil log-periodic zigzag antenna mounted on spatially varying broadband HIGP. Broadside frequency sweep.

4.4. Conclusion

Two significant conclusions can be drawn from the application of a planar log-periodic zigzag antenna to high impedance ground plane surfaces. Both conclusions counter the hypothesis that a high impedance ground plane can be used as a reflector for existing broadband surface mount antennas. However, both conclusions also suggest ways to make a broadband antenna/ground-plane work.

Applying a log-periodic zigzag antenna to the surface of a homogeneous narrowband HIGP reveals the high impedance ground plane alters the fundamental

radiating modes of the antenna. While the antenna/ground-plane pair radiates within the expected band gap of the HIGP, the antenna no longer radiates from the expected log-periodic active region. The radiation produced by a surface mount antenna on a HIGP is a function of how the antenna locally couples to the ground plane rather than a function of how the antenna behaves autonomously.

Applying a log-periodic zigzag antenna to the surface of an inhomogeneous spatially varying HIGP reveals the high frequency region of the ground plane shorts out all energy in frequencies below its active band gap. Low frequency energy cannot propagate over the high frequency elements of the ground plane and never reaches the center feeds of the planar log-periodic antenna. Energy from low frequency regions of a log-periodic surface mount antenna is lost when the transmission region of the antenna must pass over a HIGP region with a higher frequency stop band.

The conclusions suggest two possible ways to make a broadband surface mount antenna/ground-plane pair work. First, the antenna should be designed in terms of how it couples to the ground plane elements. The antenna should possibly follow the basic structure of the ground plane elements themselves. Second, a pathway or transmission region in the antenna/ground-plane pair must be maintained for low frequency energy. The antenna should possibly be made integral to the ground plane itself. Marrying the two suggestions leads to an antenna/ground-plane structure created by tying basic ground plane elements together to form larger integral radiating elements surrounded by a high impedance region.

5. Integral Antenna Designs

Chapter 4 explored using high impedance ground planes as reflectors for broadband surface mount antennas. The experiments revealed two primary characteristics dominate the interaction between the surface mount antenna and ground plane. First, coupling between the antenna and ground plane elements alters the fundamental radiating modes of the antenna. Second, broadband energy in the antenna cannot propagate over locally narrowband regions of the ground plane. One possible way to take advantage of the first and avoid the second is to construct the antenna out of the ground plane elements themselves. The resulting antenna/ground-plane structure would maximize the coupling between antenna elements and the surrounding ground plane elements, and provide a path for broadband energy to propagate through locally narrowband ground plane regions.

This Chapter explores integrated antenna/ground-plane structures. The first set of experiments explores constructing basic monopole antennas using copper tape to connect ground plane elements. Novel broadband antenna/ground-plane structures based on log-periodic principles are introduced and tested. Finally, thermal imaging techniques are used to analyze the near-field radiation characteristics of the antenna structures.

5.1. Tape Monopoles

Section 4.1.1 provides an example of previous experiments where horizontal monopole antennas are mounted over a high impedance ground plane surface [9]. The

center conductor of a coax feed was extended beyond the ground plane surface and bent over horizontally. The antenna remained physically isolated from the ground plane elements. By contrast, the following experiments create monopole antennas out of the ground plane elements themselves. The center conductor of a coax feed is extended through the ground plane dielectric substrate and soldered to one ground plane hex element on the surface. Multiple ground plane elements are then tied together with a thin strip of copper tape to create an integrated monopole antenna. See Figure 34 for an example.

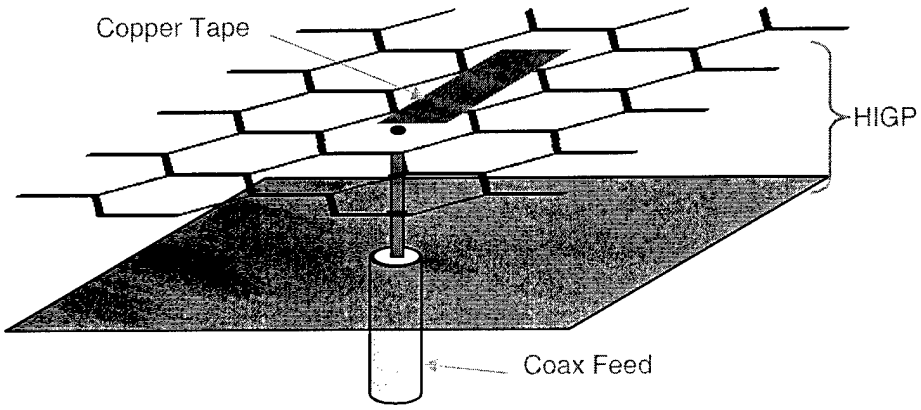

Figure 34. Copper tape monopole directly on high impedance ground plane elements.

The reported monopoles are all linear combinations of HIGP elements created on homogeneous narrowband ground planes. Each set of measurements represents a series of different length monopoles on the same ground plane. The data sets differ by whether the associated HIGP has conducting vias or not, and by the proportional scale of the HIGP elements. The relative size of the high impedance region surrounding each

monopole is also discussed. The measurements are all broadside frequency sweeps with the transmit antenna co-polarized with the antenna under test.

5.1.1. Ground Plane with Vias.

The first monopoles were created on the same narrowband HIGP plate used for the log-periodic zigzag antenna measurements reported in Section 4.2. While the ground plane has conducting vias, measurements were taken for monopoles built out of ground plane elements with and without the vias intact.

5.1.1.1. Grounded Monopoles.

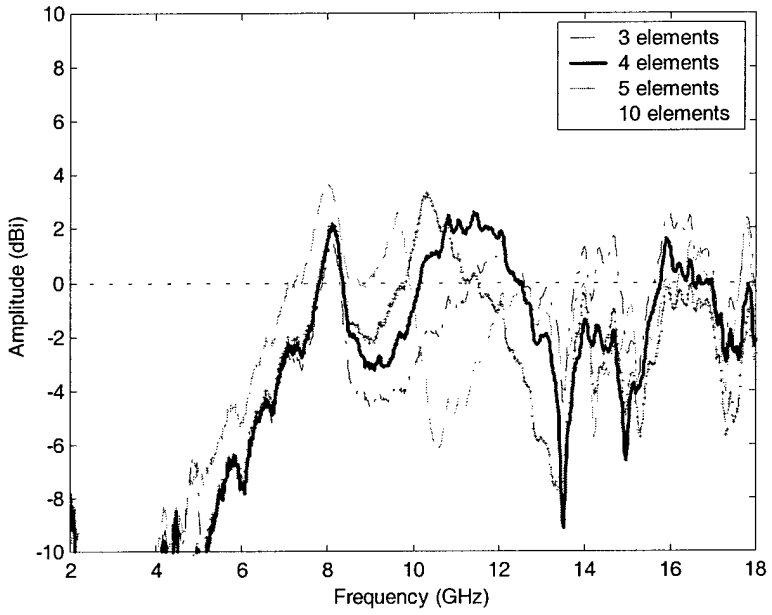

Figure 36. Copper tape monopoles coupling elements of narrowband HIGP with vias. Broadside frequency responses.

Figure 36 plots the broadside amplitude responses for monopole antennas constructed by linking three, four, five, and ten ground plane elements together with

copper tape. Each response appears to be dominated by returns from two frequency regions. One region, centered around 8-GHz, appears to behave independently of the length of the monopole. The second region changes with the length of the monopole. However, the change in the frequency band does not correspond with the relative change of the antenna length. Linking four ground plane elements together appears to provide the widest frequency response from 10 to 12 GHz.

5.1.1.2. Isolated Monopoles.

The monopoles in the previous measurement are shorted to ground for low frequencies down to DC by the conducting vias. Thus, the vias cannot remain intact for broadband operation. The above measurements were repeated after the vias directly under the monopole elements were drilled out to isolate the monopoles from the underlying ground plane.

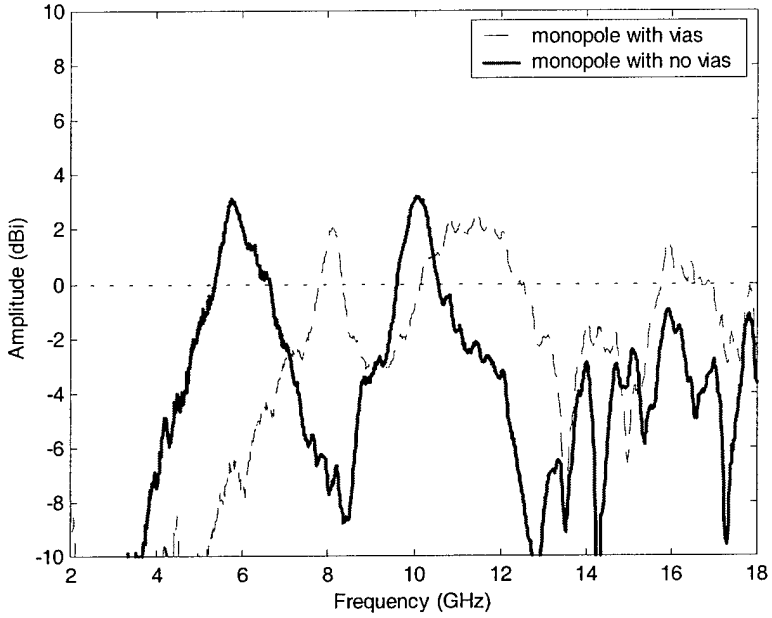

Figure 37. Four-element copper tape monopoles coupling elements of narrowband HIGP with vias. Broadside frequency responses.

Isolating the monopole elements from the rest of the ground plane leads to the response seen in Figure 37. The plot highlights the change in the response for the four-element monopole when the monopole elements are isolated from the rest of the ground plane. The isolated monopole response still shows two active bands like the normal monopole. However, the low frequency band at about 6-GHz now corresponds more closely to the expected frequency response for a quarter-wavelength monopole.

5.1.2. Ground Plane with No Vias.

Copper tape monopoles were also created on a narrowband homogeneous HIGP with no conducting vias. Other than the absence of vias, the ground plane is identical to the one used above in Section 5.1.1.

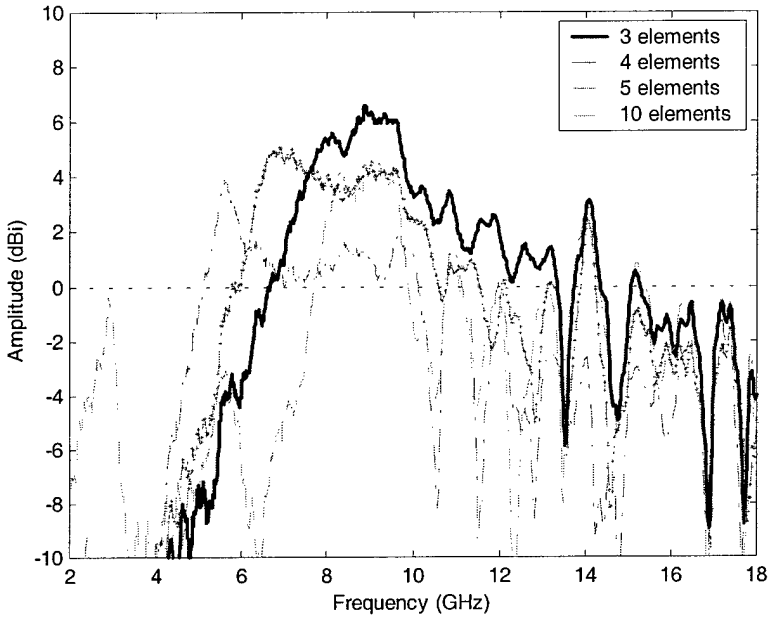

Figure 38. Copper tape monopoles coupling elements of narrowband HIGP with no vias. Broadside frequency responses.

Linking three, four, five, and ten elements of the HIGP with no vias produced the broadside frequency responses seen in Figure 38. The response peaks roughly fall at frequencies corresponding to a quarter-wavelength mode in the monopole. However, the responses extend over a much larger bandwidth for the three and four element monopoles compared to the results for the HIGP with vias in Section 5.1.1. Also, the three-element monopole appears to give the strongest and widest response for the HIGP with no vias.

5.1.3. Ground Planes with Different Stop Bands.

The monopoles reported in Sections 5.1.1 and 5.1.2, were all created on ground planes with the same sized elements. Monopoles were also created on a HIGP with physically larger elements and a correspondingly different stop band. Figure 39 shows the frequency responses for monopoles created from ground plane elements four times

larger than those used in Sections 5.1.1 and 5.1.2. The larger-scale elements produce expectedly lower-frequency responses.

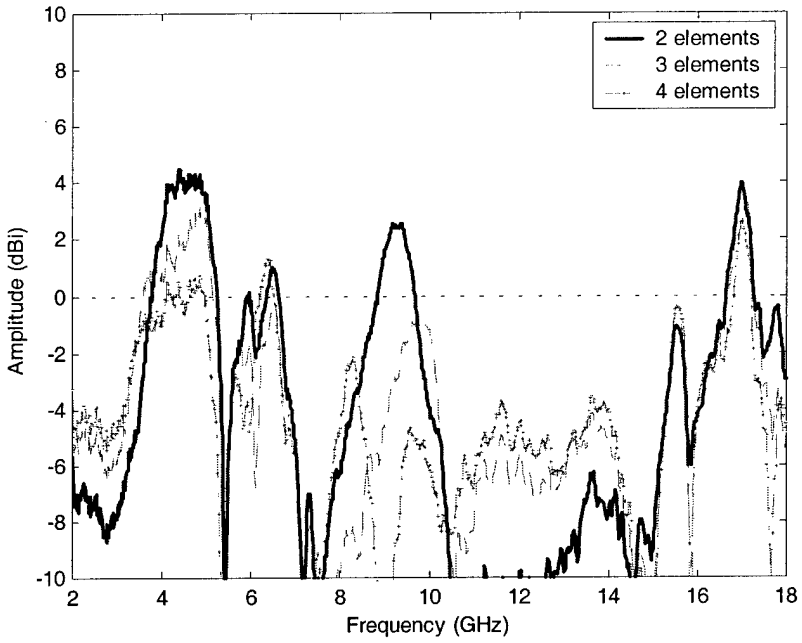

Figure 39. Copper tape monopoles coupling elements of large-scale narrowband HIGP with vias. Broadside frequency responses.

5.1.4. Surface Wave Interference.

A large region of HIGP elements surrounds the large-scale monopoles in Section 5.1.3 above. Figure 41 below shows how the frequency response changes for the two-element monopole when copper tape is used to reduce the surrounding ground plane region to one layer of HIGP elements.

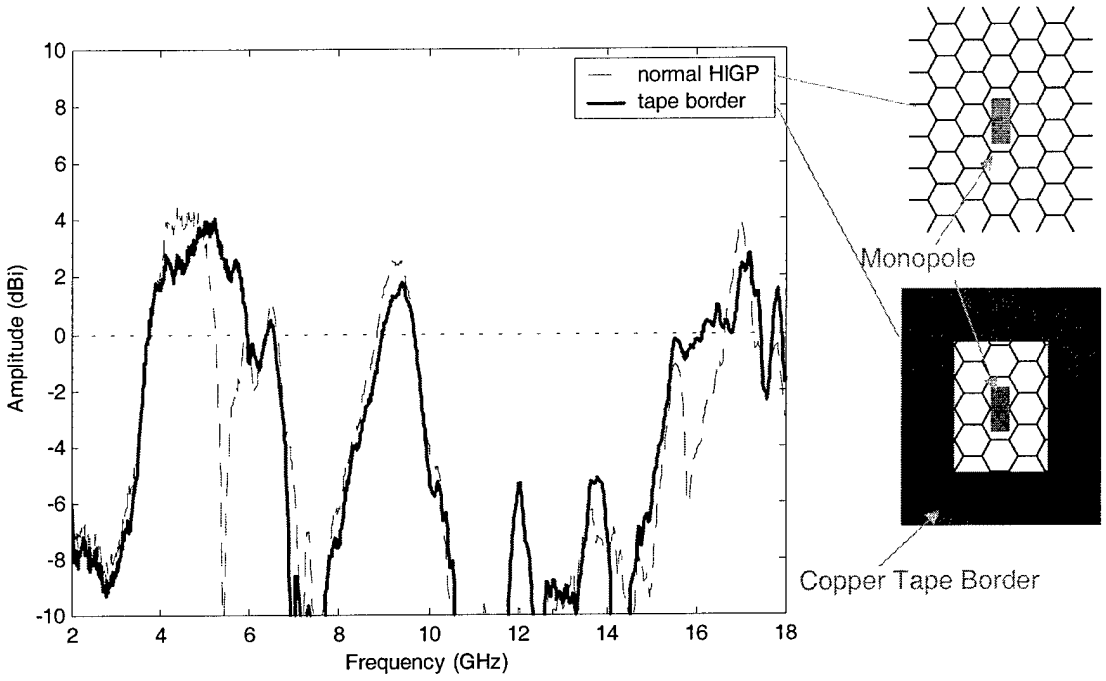

Figure 41. Two-element copper tape monopoles surrounded by differently sized ground plane regions. Broadside frequency responses.

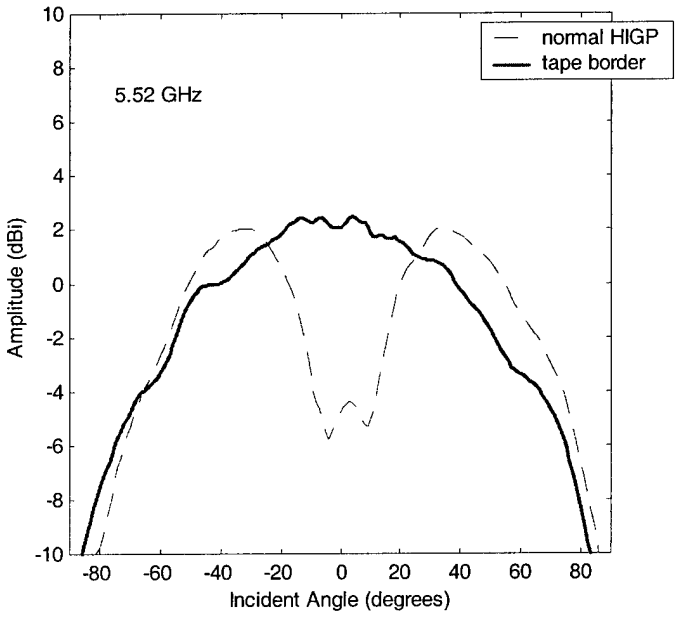

Figure 43. Two-element copper tape monopoles surrounded by differently sized ground plane regions. Co-polarized H-plane antenna patterns.

Figure 43 shows the co-polarized H-plane antenna patterns for the two-element monopoles at 5.52-GHz. The normal ground plane pattern reveals that the sharp null in the frequency response at 5.5-GHz is most likely caused by destructive interference between two scattering centers. Taping off the ground plane eliminates the null. The result suggests the null is caused by interference from surface waves or ducted waves travelling in the dielectric substrate at above resonant frequencies. The HIGP elements are changing the local coupling of the fields near the antenna edges.

Sievenpiper reported that surface waves propagate on the HIGP surface at frequencies above the ground plane band gap [9]. The above result shows that although surface waves begin to propagate on the ground plane at around 5-GHz, the ground plane elements continue to enhance the integrated antenna's response to over 6-GHz. By cropping the ground plane close to the antenna, the propagating surface waves cannot destructively interfere with the desired antenna response. Limiting the surrounding ground plane region expands the effective bandwidth of the antenna/ground-plane structure.

5.2. Log-Periodic Structures

The monopole experiments in Section 5.1 provide building blocks for a potential broadband integrated antenna/ground-plane structure. The experiments show an antenna can be formed within a HIGP by connecting actual ground plane elements together. Furthermore, changing the physical scale of the underlying ground plane elements changes the frequency band of the antenna. The experiments also suggest that using

ground plane elements without conducting vias may expand the usable bandwidth of the integral antennas. While surface wave scattering appears to be a concern for the antenna/ground-plane structures, limiting the size of the surrounding ground plane region may reduce destructive interference effects.

5.2.1. Broadband Design.

The first broadband integrated antenna/ground-plane structure is based on a simple planar log-periodic template with two oppositely phased arms having four radiating elements each and a geometric ratio of $\tau = 0.37$. The radiating elements are constructed from basic HIGP elements scaled the same as those used for the broadband reflecting HIGP design in Section 4.3.1. The original narrowband HIGP geometry forms the fundamental element, one basic element is half its size, one is twice its size, and one is four times its size. The antenna seen in Figure 44 is constructed by linking progressively larger-scale ground plane regions. The lengths of the individual radiating elements match the lengths of the same-scale monopole antennas that performed the best in Section 5.1. The lateral locations of the radiating elements match the desired log-periodic proportions as closely as possible.

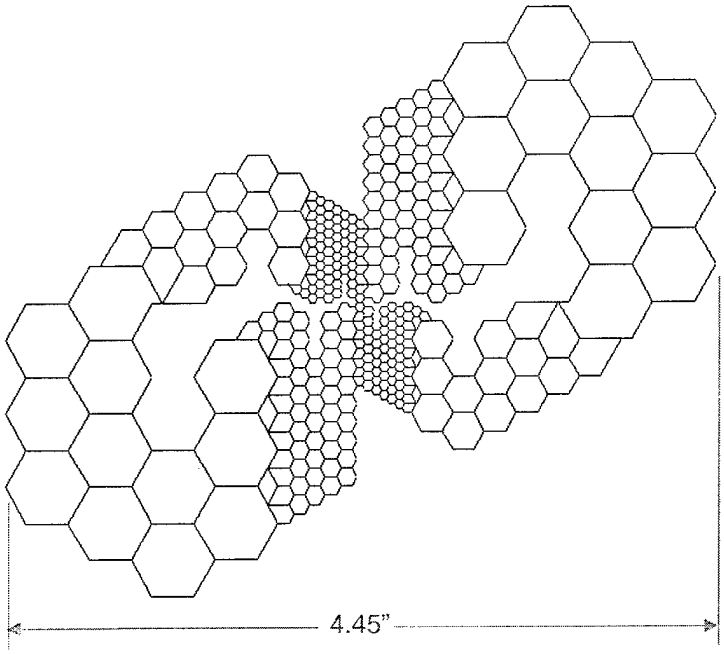

Figure 44. Planar two-arm log-periodic antenna/ground-plane structure with spatially scaled HIGP border regions.

The broadband antenna/ground-plane structure is fed with the same balanced feed applied for the zigzag antenna in Section 4.1.3. Both radiating arms are connected with semi-rigid coax to the difference outputs of a 180-degree hybrid. The region surrounding the high impedance border is PEC, making a surface mount application straightforward.

5.2.2. Broadband Performance.

Figure 46 plots the co-polarized and cross-polarized broadside frequency responses for the antenna structure with no conducting vias.

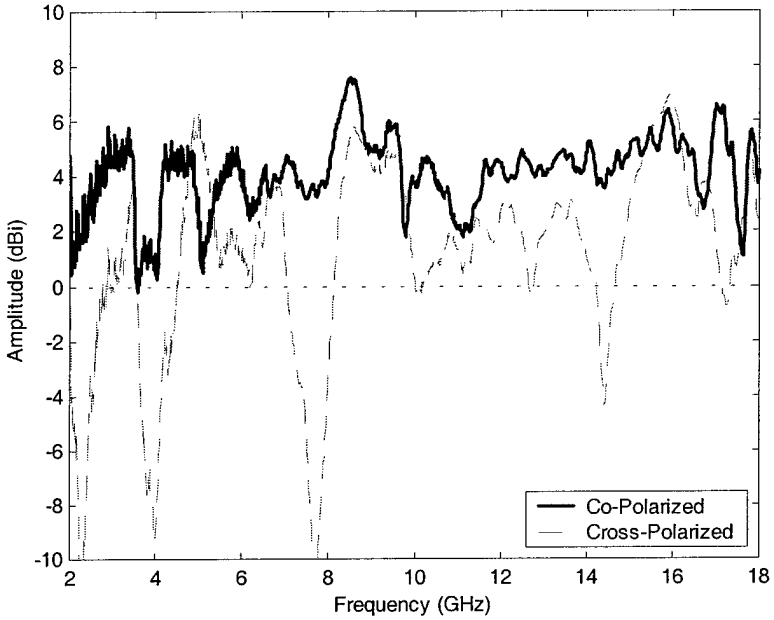

Figure 46. Planar two-arm log-periodic antenna/ground-plane structure with no vias. Broadside frequency sweeps.

The co-polarized response is relatively flat across the 2 to 18-GHz frequency band. Most importantly, the broadside gain is above 0-dBi for the entire band. The frequency responses also reveal the antenna is linearly polarized, although the cross-polarized response is high in some frequency bands. The co-polarized H-plane antenna pattern cuts for the antenna structure are also very consistent across the 2 to 18-GHz frequency band. Figure 48 provides several antenna pattern examples. All recorded pattern cuts can found in Appendix A. Figure 59.

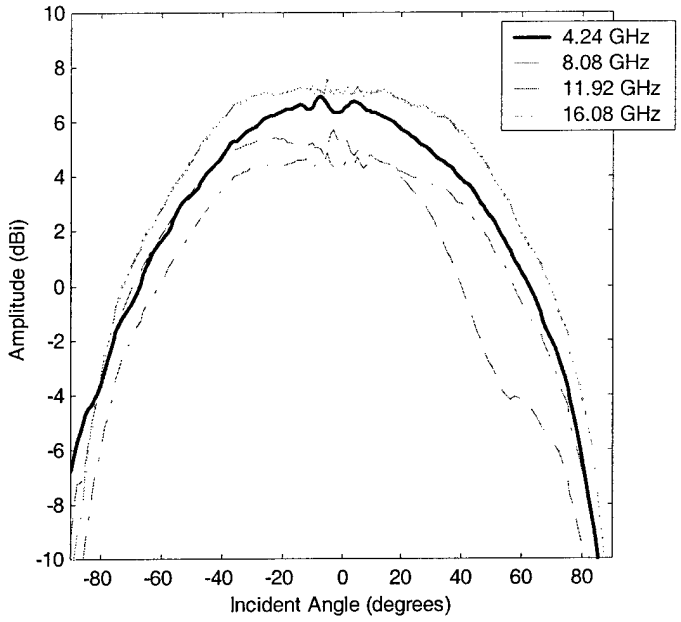

Figure 48. Planar two-arm log-periodic antenna/ground-plane structure with no vias. Co-polarized H-plane antenna pattern cuts.

An antenna/ground-plane structure with conducting vias in the high impedance region was also fabricated. Its response can be seen compared to the no-via response in Figure 39. The structure with vias did not perform as well in the mid-band region.

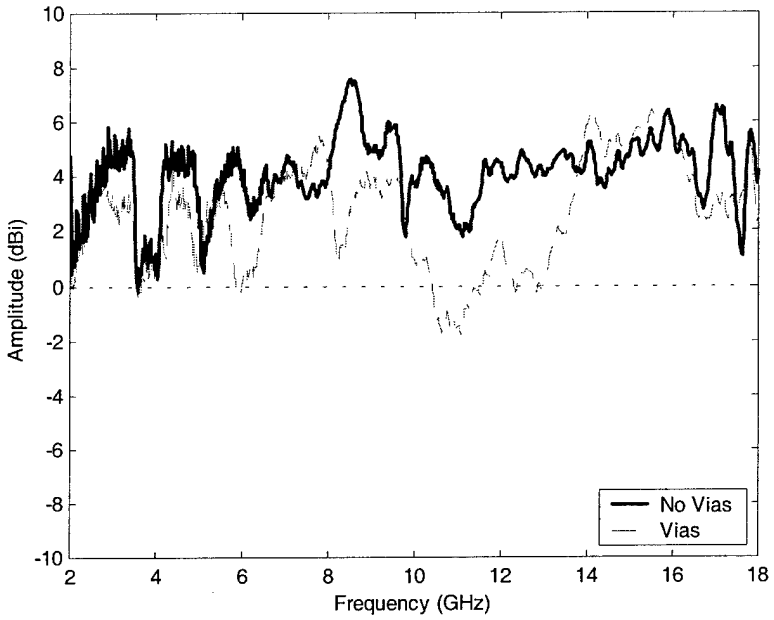

Figure 39. Planar antenna/ground plane structures with and without conducting vias in the high impedance region. Broadside frequency sweeps.

While the broadside frequency response from the structure with vias is not as good as the one with no vias, both perform better than what would be expected from a log-periodic design with only four different radiating elements. The radiating elements, acting as quarter-wavelength resonant structures, should provide strong returns at 4.1, 6.7, 11, and 18-GHz. However, the geometric ratio (τ) of 0.37 is not high enough to expect a smooth response across the 2 to18-GHz band. The following experiments attempt to help explain how the antenna/ground-plane structure provides a broadband response.

5.2.3. Experimental Analysis.

Covering different regions of the two-arm structure with copper tape reveals the structure can be simplified without reducing performance. First, the high impedance

region surrounding the radiating elements can be reduced to only one layer of high impedance elements. Second, one side of the two-arm structure and the hybrid feed can be removed without changing the basic operation. The second arm simply adds an array factor to the gain. Thus, a simplified one-arm structure was fabricated for experimental analysis. The simplified 2.5-inch square structure can be seen in Figure 41.

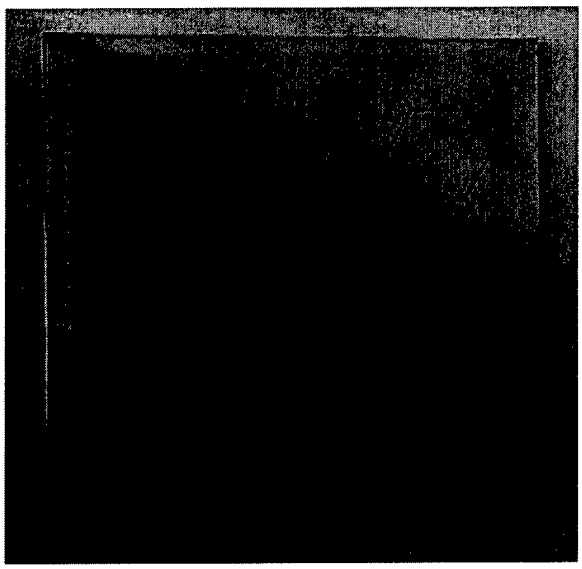

Figure 41. Simplified one-arm log-periodic antenna/ground-plane structure.

5.2.3.1. Alternative Structure Comparisons.

To help determine the role of the high impedance boundary region and help characterize the basic modes of operation for the antenna/ground-plane, two additional antenna structures were fabricated. Both structures maintain the identical log-periodic radiating arm. One replaces the surrounding high impedance region with all PEC, leaving only a 10-mil gap outlining the radiating arm. The second removes the entire surrounding region, leaving the radiating arm as a microstrip patch on a dielectric surface. Both alternative structures are pictured in Figure 43.

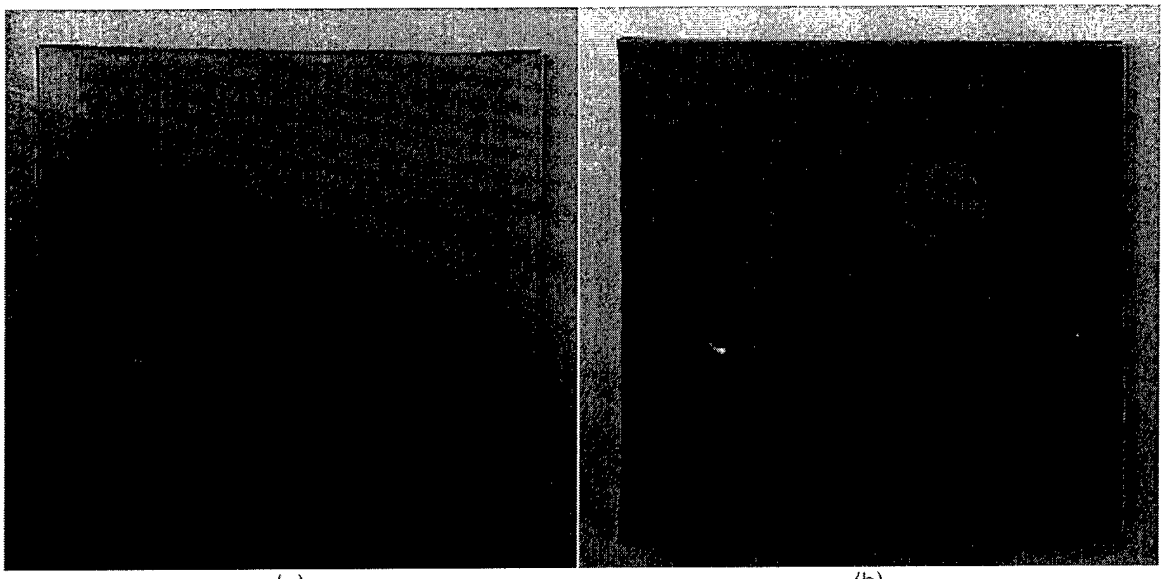

Figure 43. Log-periodic antenna structures with alternative boundary regions. (a) Radiating arm surrounded by PEC plane. (b) Radiating arm on dielectric surface, creating a microstrip patch antenna.

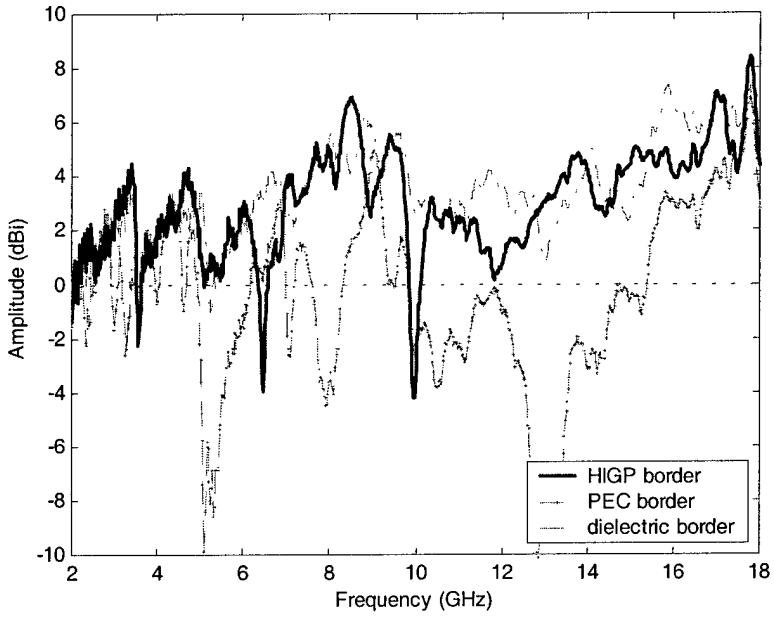

Figure 45. Simplified log-periodic antenna/ground-plane structure compared with alternative boundary regions. Broadside frequency responses.

The co-polarized, broadside frequency response curves for the three antenna structures are plotted in Figure 45. The most significant comparison is between the structure with the high impedance boundary region and the structure with the PEC boundary. The responses confirm the high impedance elements surrounding the antenna perform a valuable role in allowing the structure to radiate within a ground plane. The similarity between the high impedance boundary structure response and the response for the antenna structure over dielectric suggests the high impedance antenna/ground-plane structure is basically operating like a microstrip patch.

The primary difference between frequency responses of the high impedance boundary structure and the patch structure is the presence of nulls in the high impedance boundary response at 6.5 and 10-GHz. The antenna pattern plots in Figure 46 suggest the frequency response nulls are caused by interference from two out-of-phase radiation centers. However, the H-plane antenna patterns are relatively consistent across the rest of the frequency band. See the antenna patterns for the whole frequency band in Appendix A. Figure 53.

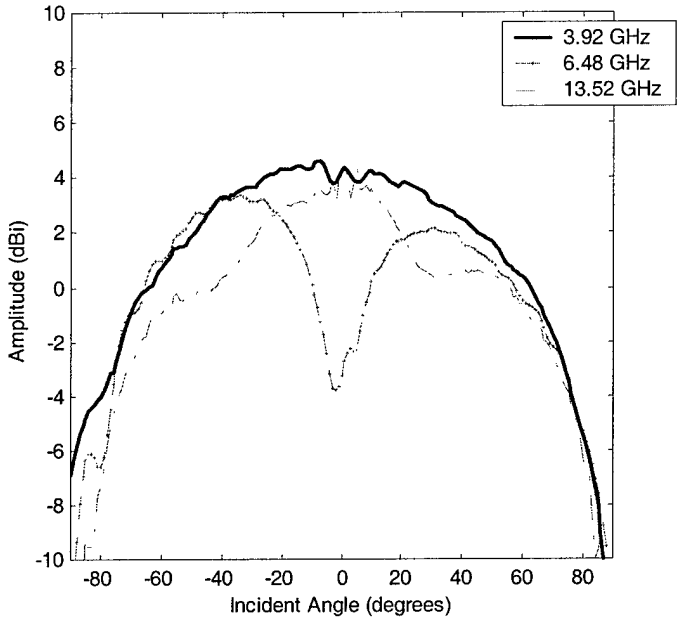

Figure 46. Simplified log-periodic antenna/ground-plane structure with high impedance boundary. Co-polarized H-plane antenna pattern cuts.

While the broadside frequency sweep measurements and antenna pattern measurements characterize how well the antenna structures receive energy, return-loss measurements provide an example of how efficiently the structures can radiate energy. Figure 44 compares the return-loss for the three alternative boundary structures. Although the plots reveal the antenna structures are not well matched to a 50Ω line, the similarity of the patch structure return-loss to the high impedance boundary structure return-loss reinforces their mutual mode of operation.

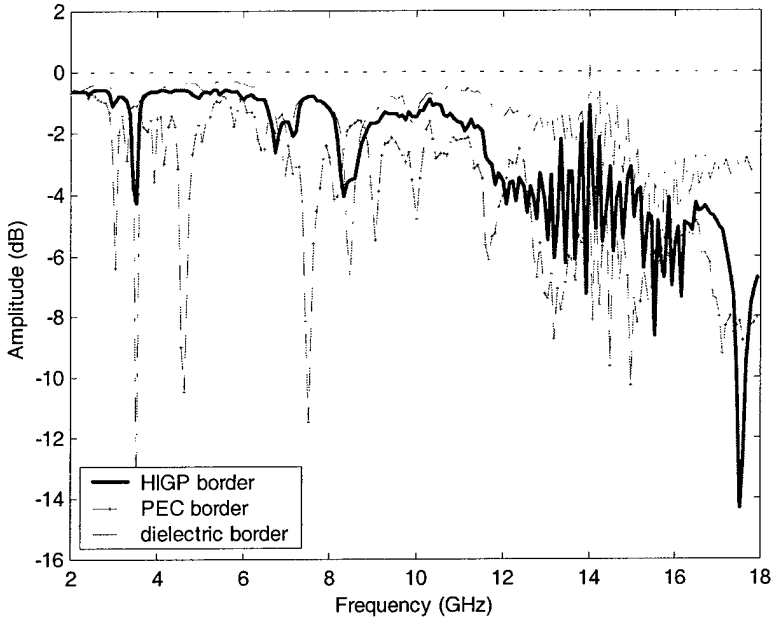

Figure 44. Simplified log-periodic antenna/ground-plane structure with alternative boundary regions. Return-loss responses.

5.2.3.2. Thermal Imaging Analysis.

Thermal imaging technology provides a novel analysis tool well suited for the planar antenna structures compared above. The technique creates an image of the near-field tangential electric fields radiating from the antenna structure. The image is created by placing a thin sheet of resistive material above the antenna surface, exciting the antenna with a single-frequency RF source, and recording the heating pattern with a thermal imager.

The restive film is rated at 1000 ohm/square and is held above the antenna surface on a 1/16-inch thick sheet of Styrofoam. The low resistivity of the film and its separation from the antenna surface help ensure the radiation characteristics of the antenna are not perturbed. Also, return-loss measurements with and without the resistive film present

showed little-to-no effect on the antenna's performance. The thermal images are recorded by an *Inframetrics,* Model 760 IR Imaging Radiometer.

The images in Figure 46 highlight how thermal analysis can contrast and compare the radiating modes of the different antenna structures.

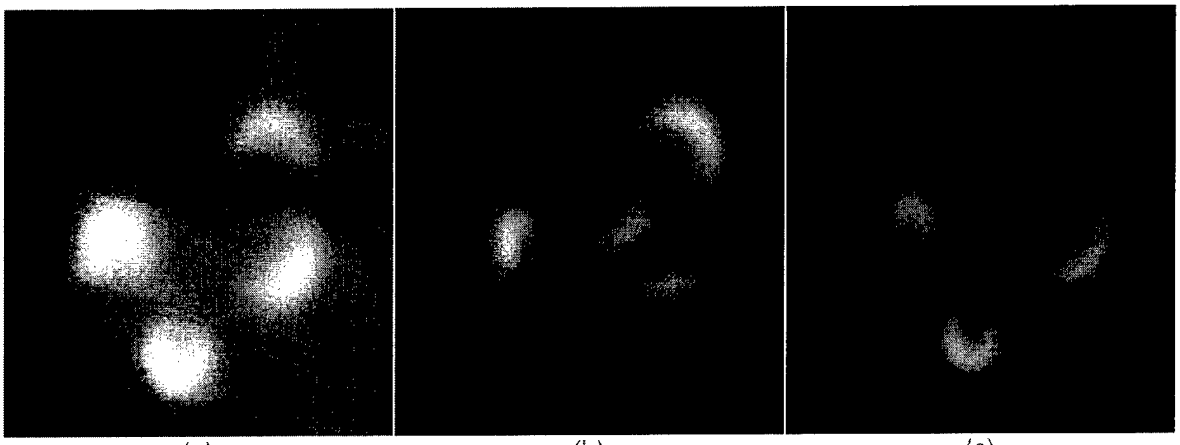

Figure 46. Thermal images of simplified antenna/ground-plane structure with alternative boundary regions radiating at 3.5-GHz. (a) With high impedance boundary. (b) With PEC boundary. (c) On dielectric only.

The images clearly show how the antenna structure with the high impedance border region radiates in the same mode as the patch structure at 3.5-GHz. The same relationship also held for other sampled frequencies. The difference of the image created by the antenna surrounded by PEC is also significant. The contrast between the radiating modes of the PEC and high impedance boundary regions emphasizes the isolation provided by the high impedance elements.

The thermal imaging technique was also able to provide some insight into how the log-periodic antenna structure achieves its broadband behavior.

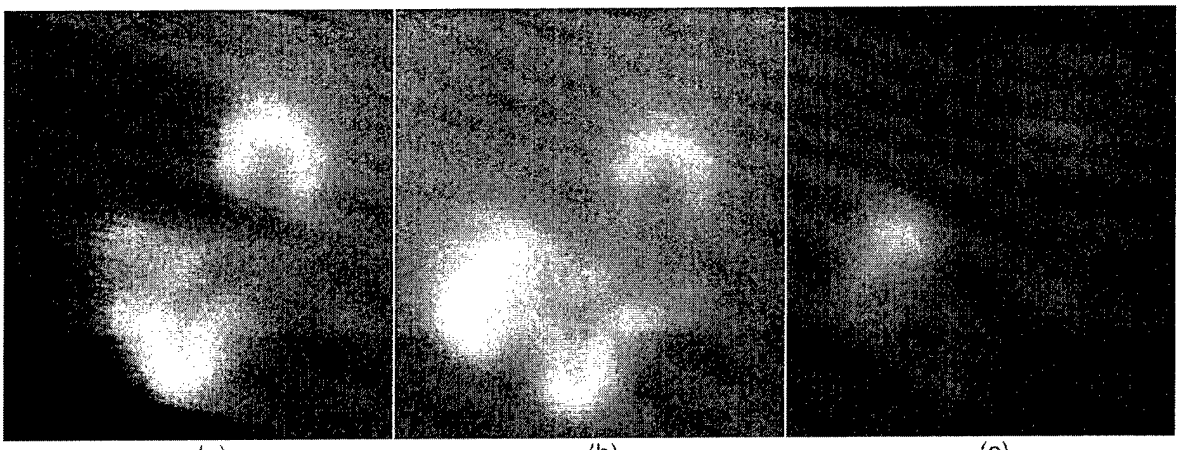

Figure 48. Thermal images of simplified antenna/ground-plane structure with high impedance boundary region. (a) Radiating at 2.0246-GHz. (b) Radiating at 2.6331-GHz. (c) Radiating at 3.0-GHz.

The thermal images recorded for the high impedance boundary antenna in Figure 48 give an example of how quickly the radiating modes of the structure can change. While the frequency shifted from 2 to 2.6 to 3-GHz in the example, more subtle changes can be detected for frequency shifts of only a few MHz. The multi-faceted geometry of the antenna structure appears to allow many more resonant modes than expected from the simple underlying log-periodic design.

5.3. Conclusion

While applying thin planar antennas to the surface of high impedance ground planes fails to create a broadband response, constructing an integral antenna/ground-plane structure can. Linking basic ground plane elements together to form larger radiating elements maximizes the coupling between the resulting antenna and the surrounding ground plane. Also, removing the conducting vias from the coupled

elements allows broadband energy to propagate through locally narrowband ground plane regions

Although narrowband by nature, copper tape monopoles coupling HIGP elements offer a wide range of possible resonant frequency bands. The resonant frequency is only dependent on the scale of the basic high impedance elements and the number of ground plane elements linked together. The monopole antenna structures are susceptible to surface wave interference at frequencies above the resonant frequency of the underlying ground plane. However, eliminating the conducting vias and limiting the size of the surrounding ground plane region expands the usable bandwidth.

Larger broadband structures can also be designed by linking spatially scaled radiating elements and ground plane regions based on an underlying log-periodic template. The resulting antenna/ground-plane structure behaves like a multi-mode microstrip patch. The faceted design provides multiple discontinuities to couple multiple resonant modes, effectively de-tuning the log-periodic structure. The surrounding high impedance elements provide the aperture. The high impedance boundary isolates the radiating elements from the larger PEC ground plane. Also, the floating boundary elements help form a voltage potential across the radiating elements allowing energy to be coupled in.

6. Conclusions

6.1. Final Remarks

In the far field, the high impedance ground plane behaves like a bulk effective medium with a reflection coefficient of +1 and an ability to suppress surface wave propagation within a certain frequency stop-band. The HIGP maintains its high impedance characteristics as long as the ground plane elements remain very small compared to the wavelength of the incident energy, and as long as the effective ground plane region is large compared to individual elements.

However, the high impedance ground plane does not operate as a simple reflector for an applied surface mount antenna. The high impedance elements of the ground plane alter the fundamental radiating modes of antenna elements placed on or near the ground plane surface. Interactions between the antenna elements and the underlying ground plane elements overwhelm the original operating modes of the antenna. The antenna and ground plane pair radiates as a function of how the antenna elements couple high impedance elements together. Also, broadband energy cannot propagate over locally narrowband regions of a spatially varying HIGP. The high frequency region of the ground plane shorts out energy from low frequency regions of the applied antenna.

Integrating a broadband antenna design into the basic structure of the ground plane itself provides an opportunity to achieve broadband behavior. The radiating element becomes a microstrip patch antenna while the surrounding high impedance

ground plane elements form an aperture isolating the patch from the surrounding PEC ground plane. Broadband operation is achieved because the hex-pattern ground plane geometry forms a multi-faceted radiating element. The resulting discontinuities in the radiating element allow multiple resonant modes to form, generating a broadband response.

The radiating ground plane antenna shows great potential for broadband surface-mount antenna applications. Although the reported design does not radiate efficiently across the entire frequency band, it is ideal for broadband receive-only deployment. Also, the design remains open to optimization. Both the broadband patch element and the surrounding high impedance boundary can be tuned to improve the input impedance and broadband radiating characteristics.

6.2. Recommendations

Three areas of this thesis research hold significant potential for continuing study. First, the introduction of the broadband integrated antenna/ground-plane structure provides an opportunity for optimization and analysis. Second, the log-periodic zigzag microstrip antenna itself holds potential for further analysis and application. Third, the HIGP characterization measurements revealed several potential techniques for applying broadband spatially varying high impedance ground plane structures to RCS reduction applications.

6.2.1. Integrated Antenna/ Ground-Plane Structures.

The integrated antenna/ground-plane structure leaves many variables open for optimization. A concentrated study of the microstrip patch design by itself is needed to fully characterize its multi mode behavior and optimize its broadband performance. Both experimental and electromagnetic simulation techniques could provide insight. Also, the geometry of the high impedance boundary and the existence and placement of conducting vias can be explored. Furthermore, the concept of a high impedance isolation boundary can be applied to other existing microstrip patch designs such as square, circular, triangular, or arrayed patches.

Direct application of the radiating ground plane design can also be studied. Conformal designs can be evaluated for real world applications. Also, the structure holds great potential for low observable applications. An experiment could evaluate how the integrated antenna/ground-plane structure affects the radar cross section of a body compared to existing antenna structures in the same frequency band.

6.2.2. Log-Periodic Zigzag Microstrip Antenna.

The log-periodic zigzag antenna is ideally suited for further study and electromagnetic simulation. Further analysis and full characterization can lead to a simple design methodology for many applications. The design can also be studied for conformal applications.

6.2.3. RCS Reduction Applications.

The bulk material properties of the high impedance ground plane remain desirable for RSC reduction applications. A spatially scaled HIGP design could take advantage of the locally narrowband nature of the ground plane regions to create an effectively broadband diffraction grating. For a given frequency of incident energy, some regions of the ground plane will be resonant and others will not. The resulting interference pattern between energy reflected in phase and out-of-phase from the different ground plane regions could create a grating lobe and reduce the expected specular reflection response.

A second application of spatially varying HIGP regions could be broadband surface wave suppression. Straightforward application of side-by-side bands of differently scaled HIGP regions could provide a practical broadband technique for reducing creeping waves and the scattering caused by travelling surface waves.

Appendix A

a. GTRI focused beam arch plane wave reflection measurements

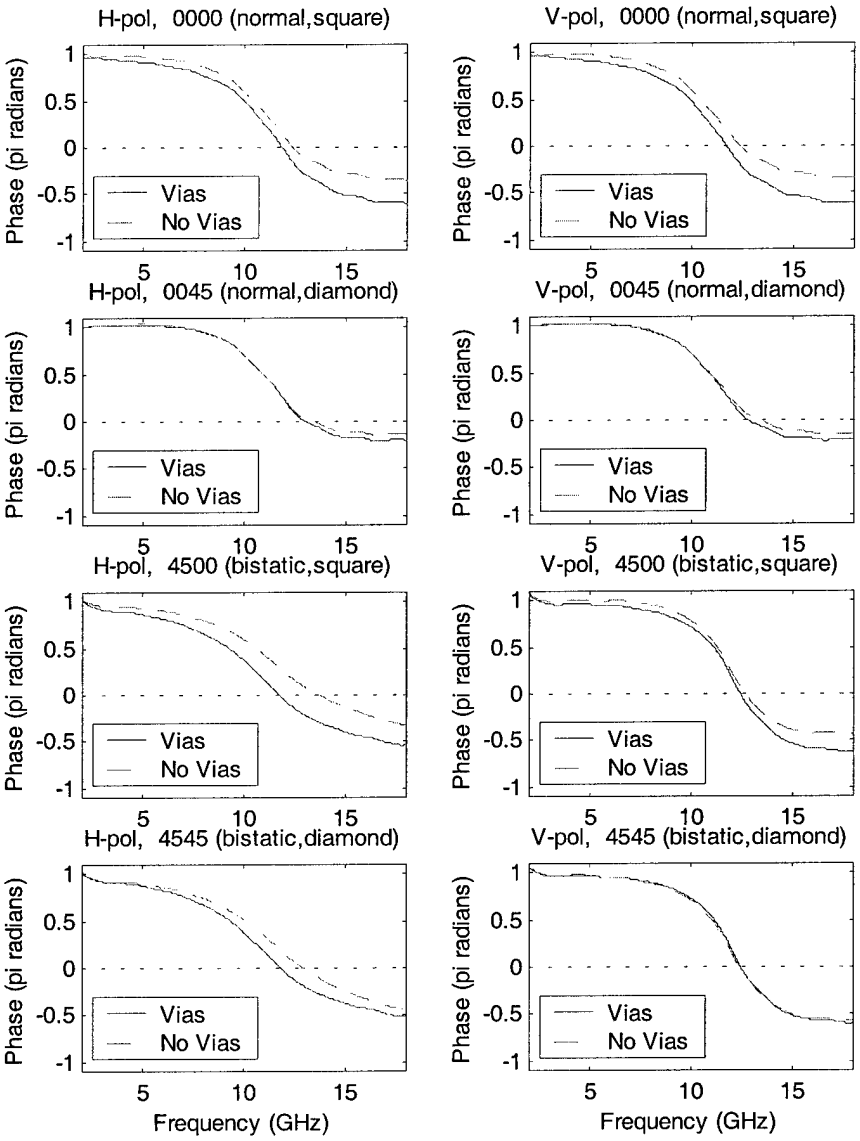

Figure 54. HIGP phase responses from plane wave measurements at different sample orientations. Horizontal/Vertical polarizations, monostatic/bistatic reflection angles, square/diamond azimuth angles. Refer to Section 3.2 for details.

b. Planar antenna/ ground-plane structure, H-plane pattern cuts.

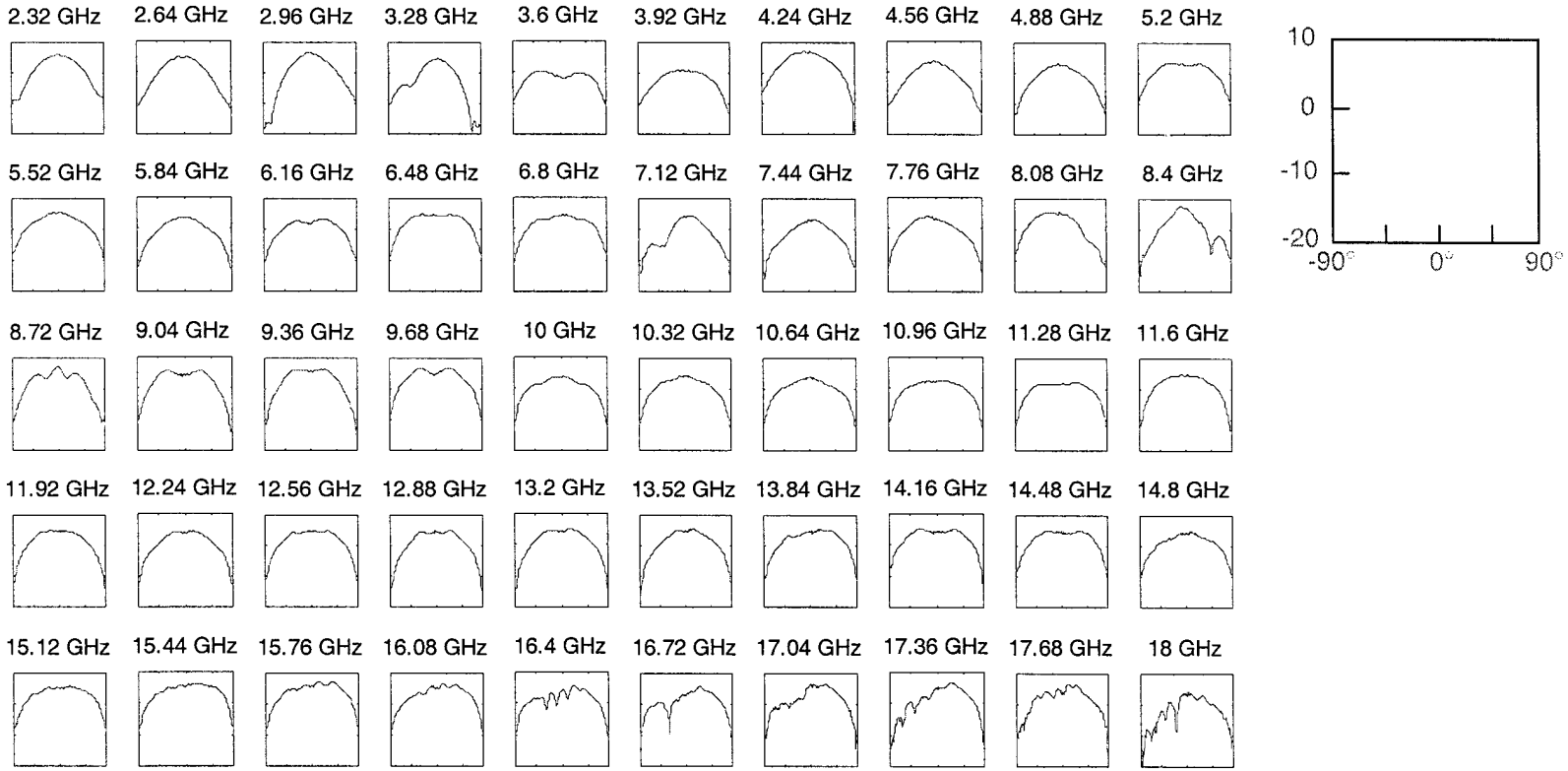

Figure 59. Planar two-arm log-periodic antenna/ground-plane structure with no vias. Co-polarized H-plane antenna pattern cuts.

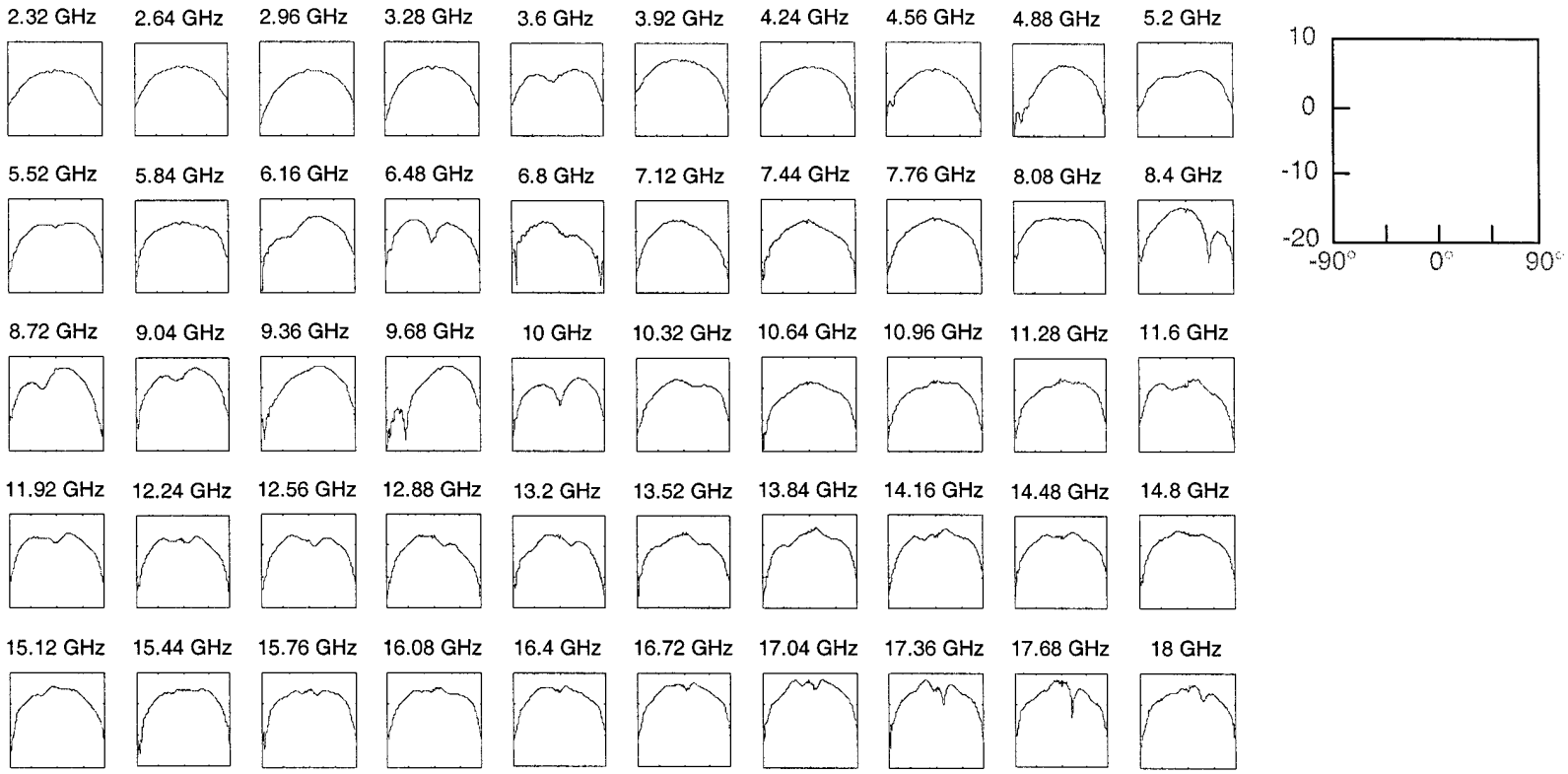

Figure 53. Simplified log-periodic antenna/ground-plane structure with HIGP boundary. Co-polarized H-plane antenna pattern cuts.

References

[1] E. Yablonovitch, "Inhibited Spontaneous Emission in Solid State Physics and Electronics," *Physical Review Letters*, vol. 58, pp. 2059-2062, May 1987.

[2] E. Hecht, *Optics*. 3rd edition, Massachusetts: Addison Wesley Longman, 1998.

[3] E. Yablonovitch, T. J. Gmitter, and K. M. Leung, "Photonic Band Structure: The Face-Centered Cubic Case Employing Nonspherical Atoms," *Physical Review Letters*, vol. 67, pp. 2295-2298, Oct. 1991.

[4] M. Thevenot, C. Cheype, A. Reineix, and B. Jecko, "Directive Photonic-Bandgap Antennas," *IEEE Trans. Microwave Theory Tech.*, vol.47, no. 11, pp. 2115-2122, Nov. 1999.

[5] K. Schloer, *Antenna Gain Enhancement Using a Photonic Band Gap Reflector*, MS thesis, AFIT/GE/ENG/99M-26. School of Engineering, Air Force Institute of Technology, Wright-Patterson AFB OH, Mar. 1999.

[6] D. Sievenpiper, E. Yablonovitch, J. Winn, S. Fan, P. Villeneuve, J. Joannopoulos, "3D Metallo-Dielectric Photonic Crystals with Strong Capacative Coupling between Metallic Islands," *Physical Review Letters*, vol. 80, pp. 2829-2832, Mar. 1998.

[7] M. P. Kesler, J. G. Maloney, and B. L. Shirley, "Antenna design with the use of photonic bandgap materials as all dielectric planar reflectors," *Microwave and Optical Technology Letters*, vol. 11, pp. 169-174, Mar. 1996.

[8] D. F. Sievenpiper, M. E. Sickmiller, and E. Yablonovitch, "3D Wire Mesh Photonic Crystals," *Physical Review Letters,* vol. 76, pp. 2480-2483, Apr. 1996.

[9] D. Sievenpiper, *High-Impedance Electromagnetic Surfaces*, Ph.D. dissertation, University of California at Los Angeles, Los Angeles, CA, 1999.

[10] D. Sievenpiper, L. Zhang, R.F. J. Broas, N. G. Alexopolous, and E. Yablonovitch, "High-Impedance Electromagnetic Surfaces with a Forbidden Frequency Band," *IEEE Trans. Microwave Theory Tech.*, vol. 47, no. 11, pp. 2059-2074, Nov. 1999.

[11] R. H. DuHamel and D. E. Isbell, "Broadband Logarithmically Periodic Antenna Structures," *1957 IRE National Convention Record*, pt. 1, pp. 119-128.

[12] R. H. DuHamel and F. R. Ore, "Logarithmically Periodic Antenna Designs," *IRE National Convention Record*, pt. 1, pp. 139-152, 1958.

[13] M. Saville, *Investigation of Conformal High-Impedance Ground Planes*, MS thesis, AFIT/GE/ENG/00M-17. School of Engineering, Air Force Institute of Technology, Wright-Patterson AFB OH, Mar. 2000.

Vita

Lt. Keven J. Golla was born and raised in San Antonio, Texas. He graduated from High School in Kerrville, Texas, and attended Trinity University in San Antonio for three years where he studied Math and Physics. He enlisted in the Air Force in 1992 as a Systems Repair Technician. He was assigned to the Technical Operations Division of the Air Force Technical Applications Center (AFTAC) at McClellan AFB, California.

In 1994, Lt. Golla was selected for the Airman Education and Commissioning Program and attended the University of Texas in Austin. He completed a Bachelor of Science Degree in Electrical Engineering and was commissioned a Second Lieutenant in 1997.

Lt. Golla was assigned as a Developmental Electrical Engineer at the Air Force Research Laboratory, Directed Energy directorate, High Power Microwave Applications branch, Kirtland AFB, New Mexico. There he served as a Deputy Program Manager developing innovative electromagnetic warfare technology from December 1997 through August 1999.

In August 1999, Lt. Golla entered the School of Engineering, Air Force Institute of Technology, to begin a Master of Science program in Electrical Engineering. Upon Graduation in March 2001, Lt. Golla was assigned to Air Force Research Laboratory, Sensors directorate at Wright Patterson AFB, Ohio.

REPORT DOCUMENTATION PAGE

Form Approved
OMB No. 0704-0188

1. REPORT DATE (DD-MM-YYYY)	2. REPORT TYPE	3. DATES COVERED (From - To)
March 2001	Master's Thesis	June 2000 - March 2001

4. TITLE AND SUBTITLE
BROADBAND APPLICATION OF HIGH IMPEDANCE GROUND PLANES

5a. CONTRACT NUMBER

5b. GRANT NUMBER

5c. PROGRAM ELEMENT NUMBER

6. AUTHOR(S)
Golla, Keven J., 1Lt, USAF

5d. PROJECT NUMBER

5e. TASK NUMBER

5f. WORK UNIT NUMBER

7. PERFORMING ORGANIZATION NAME(S) AND ADDRESS(ES)
Air Force Institute of Technology
Graduate School of Engineering and Management (AFIT/EN)
2950 P Street, Building 640
WPAFB OH 45433-7765

8. PERFORMING ORGANIZATION REPORT NUMBER
AFIT/GE/ENG/01M-11

9. SPONSORING/MONITORING AGENCY NAME(S) AND ADDRESS(ES)
Attn: Dr Stephen Schneider
AFRL/SNRP
2241 AVIONICS CIRCLE
WPAFB OH 45433
COMM: (937) 255-4120

10. SPONSOR/MONITOR'S ACRONYM(S)

11. SPONSOR/MONITOR'S REPORT NUMBER(S)

12. DISTRIBUTION/AVAILABILITY STATEMENT
Approved for Public Release, Distribution Unlimited

13. SUPPLEMENTARY NOTES
AFIT Technical POC: Peter J Collins, Maj, AFIT/ENG
peter.collins@afit.edu

14. ABSTRACT
Electrical conductors have long been the only materials available to antenna designers for reflecting structures. However, recently reported high impedance ground plane (HIGP) structures offer an alternative by creating image currents and reflections, within a limited frequency stop-band, that are in-phase with a source rather than out-of-phase as for a perfect electric conducting (PEC) surface. Also, the high impedance structures suppress surface waves while surface waves propagate on PEC surfaces. This research explores broadband antenna applications for HIGP structures. A broadband surface mount antenna is applied to both a homogeneous narrowband HIGP and a spatially varying broadband HIGP design. Measurements reveal the ground plane alters th fundamental radiating modes of the antenna and show high frequency regions of the ground plane short out low frequency energy in the antenna. Novel broadband integrated antenna/ground-plane structures are also introduced and analyzed. Basic high impedance elements are linked to form larger broadband antenna elements within the ground plane itself. The structure provides a passive-receive capability over a 9 to 1 bandwidth, is very light and thin, and offers straightforward flush-mounted integration on PEC surfaces.

15. SUBJECT TERMS
High impedance ground plane, broadband surface mount antenna, integrated antenna/ground-plane structure, conformal antenna, microstrip antenna, broadband patch antenna, surface wave suppression.

16. SECURITY CLASSIFICATION OF:			17. LIMITATION OF ABSTRACT	18. NUMBER OF PAGES	19a. NAME OF RESPONSIBLE PERSON
a. REPORT	b. ABSTRACT	c. THIS PAGE			Peter J. Collins, Maj, AFIT/ENG
U	U	U	UU	108	19b. TELEPHONE NUMBER (Include area code) (937) 255-3636, ext 4612